AD-A129 792 COVERAGE PREDICTIONS AND SELECTION CRITERIA FOR SATELLITE CONSTELLATIONS(U) ROYAL AIRCRAFT ESTABLISHMENT FARNBOROUGH (ENGLAND) J G WALKER DEC 82 1/1

UNCLASSIFIED RAE-TR-82116 DRIC-BR-87935 F/G 22/1 NL

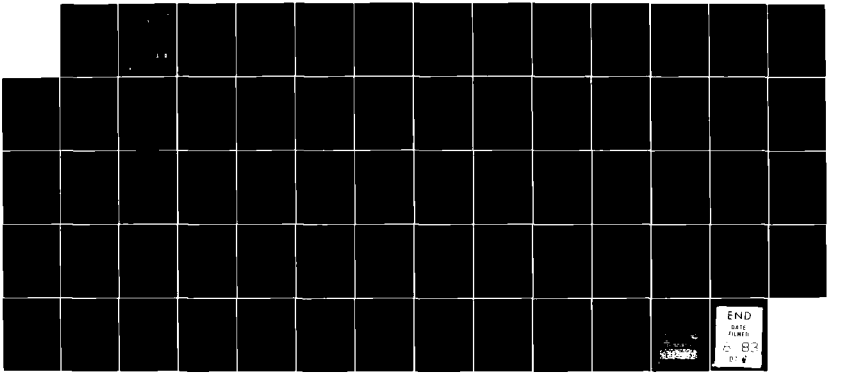

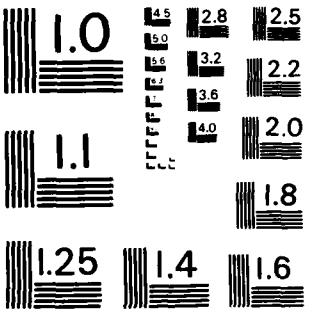

ROYAL AIRCRAFT ESTABLISHMENT

*

Technical Report 82116

December 1982

COVERAGE PREDICTIONS AND SELECTION CRITERIA FOR SATELLITE CONSTELLATIONS

by

J. G. Walker

*

Procurement Executive, Ministry of Defence
Farnborough, Hants

UDC 629.194.2 : 629.19.077.3

ROYAL AIRCRAFT ESTABLISHMENT

Technical Report 82116

Received for printing 2 December 1982

COVERAGE PREDICTIONS AND SELECTION CRITERIA FOR SATELLITE CONSTELLATIONS

by

J. G. Walker

SUMMARY

To assist in the prediction of the Earth-coverage capabilities of large constellations of satellites, studies have been conducted of patterns based on regular tesselations of a plane surface and of others based on regular polyhedra. This work has identified trends associated with increasing numbers of satellites and degrees of coverage, permitting extrapolation from the known capabilities of smaller satellite constellations. An investigation of selection criteria has emphasised the importance of the minimum inter-satellite distance, which provides a particularly convenient criterion for use in preliminary studies, and this in turn has been used in an examination of some non-uniform orbital patterns, which has suggested an improved method of synthesising such patterns. Results obtained have been discussed with reference to the requirements of the GPS navigation satellite system.

Departmental Reference: Space 621

LIST OF CONTENTS

1 INTRODUCTION

Methods of achieving continuous coverage of the whole surface of the Earth by optimised constellations of satellites have been studied by various organisations for more than 20 years, this in support of a variety of satellite missions such as communications, navigation and surveillance. At RAE, the author has made a number of studies in this field, many of which were collected in two Reports issued in 1970 and 1977. This present Report summarises further studies performed during the period 1977-1982.

The 1970 Report[1] described analyses which had been made, using hand methods, of two types of circular orbit constellations which were described as star patterns and delta patterns respectively; by the time it was issued, work had started on a computer program (COCO) needed for further analysis of the more complex delta patterns. A 1971 paper[2] summarised that report, including corrected results in a few cases where early computer runs had shown their need. A brief paper[3] issued in 1973 contained summarised results of comprehensive computer studies of delta patterns containing up to 15 satellites providing up to four-fold continuous coverage of the whole Earth's surface, and described the method of classifying patterns which had been adopted for use with the computer program. The 1977 Report[4] provided fuller details of these studies, and of later extensions to cover delta patterns of up to 25 satellites providing up to seven-fold continuous coverage of the whole Earth's surface; it also contained an analysis of the Earth-tracks followed by delta patterns, including a method of identifying those patterns which would follow a single repetitive Earth-track at a particular orbital period, and identified certain series of patterns which both followed single non-self-crossing Earth-tracks and included many of the patterns providing the highest standards of coverage. This Report also described the program COCO used for coverage studies.

In Refs 1 and 2 star patterns were defined as consisting of multiple orbits (with equal numbers of equally-spaced satellites in each) sharing two common points of intersection (which may be considered as the poles of a reference plane), with all ascending nodes (with respect to the reference plane) lying in one 180° arc of the reference plane and all descending nodes in the other, and with equal intervals between adjacent ascending nodes; delta patterns were also defined as consisting of multiple orbits with equal numbers of equally-spaced satellites in each, but with all orbits having the same inclination δ to a reference plane and with ascending nodes evenly spaced around the reference plane. Later reports and papers concentrated on the delta patterns, which were found to give generally superior results. Ref 3 introduced the identification code T/P/F for delta patterns which had been adopted when writing the computer program COCO; here T is the total number of satellites in the pattern, P is the number of equally-spaced orbital planes of inclination δ between which they are equally divided, and F is a measure of the phase difference between satellites in adjacent planes such that, when a satellite in one plane reaches its ascending node, one of the satellites in the adjacent plane having a more easterly ascending node is F units of $360^\circ/T$ past its ascending node. For a delta pattern P may be any factor of T, including 1 and T, and F may have any integer value from 0 to (P - 1).

This series of reports and papers discussed standards of coverage provided by the various satellite patterns in terms (using nomenclature adopted in Ref 4) of a parameter R_n, the angle subtended at the centre of the Earth by the radius of the circumcircle of three sub-satellite points which encloses $(n - 3)$ other sub-satellite points. It was demonstrated (and an alternative form of demonstration is given in section 2.2 of this Report) that the centre of such a circumcircle is the locally least-favoured point for seeing at least n satellites at maximum elevation above the horizon, system requirements usually being written in terms of a minimum elevation angle. The quantity $R_{max,n}$ (with a small 'm') was defined as the instantaneous value of the largest circumcircle radius in the constellation for degree of coverage n, and δ as the common inclination of the orbital planes of the constellation to its reference plane. The internal configuration of the constellation would vary systematically during an orbital period, and $R_{Max,n}$ (with a capital 'M') was defined as the largest value of $R_{max,n}$ during a complete orbital period, for any particular inclination δ. $R_{Max,n}$ should preferably be as small as possible, in order to make the minimum elevation angle as large as possible (with satellites at a given altitude) or to permit the satellite altitude to be as low as possible (for a given minimum elevation angle); by varying the common inclination δ of the orbital planes it is possible to find an inclination δ_{opt} at which $R_{Max,n}$ has a minimum value, defined as $R_{MAX,n}$ (with 'MAX' in capitals).

The main objective was generally taken to be the identification of the pattern which, for a particular value of T (and perhaps also of P), could provide the smallest value of $R_{MAX,n}$. However, it was considered that the minimum value of the inter-satellite distance D was also of some significance (as discussed in section 2.3), with any value less than about 3° probably being unacceptable, and zero minimum separation almost certainly so; hence values of D were also calculated. In similar manner to $R_{max,n}$, D_{min} was defined as the smallest instantaneous value of the inter-satellite distance occurring in the constellation; D_{Min} as the smallest such value during a full orbital period; and D_{MIN}, with corresponding inclination $\delta_{opt,D}$, as the largest value of D_{Min} which could be found by varying the inclination δ. In Refs 1 to 4 only values of D_{Min} at δ_{opt} were calculated and presented with the values of $R_{MAX,n}$; later in 1977, however, after preparation of Ref 4, values of D_{MIN} were investigated, and the results were described briefly in a paper[5] issued in 1978 and are presented more fully here.

An appendix to Ref 4 discussed the relevance of its contents to navigation satellite systems, such as the US GPS system (using Navstar satellites) which was then expected to be a three-plane 24-satellite system. In 1980 it became known that the initial GPS system would contain only 18 active satellites, in a pattern still to be determined; as 18-satellite delta patterns had been examined in 1974-5 using the program COCO, but only some of these results had been listed in Ref 4 and commented on in its Appendix A, the relevant computer printouts were re-examined and an unpublished RAE note[6] on the findings was prepared. Information was subsequently received on US studies of some non-uniform 18-satellite patterns; a brief further study of such non-uniform patterns was made, resulting in another unpublished RAE note[7].

The present writer had, during preparation of Ref 1, considered the possibility of obtaining guidance for the study of satellite constellations from a study of the regular polyhedra, and to this end examined Critchlow's book[9] on the characteristics of regular and semi-regular polyhedra and tesselations. At that time no information directly relevant to the study of satellite constellations was identified, though it was recognised that a regular polyhedron represents the most 'efficient' possible distribution of the relevant number of vertices (or satellites), which cannot be matched on a worst-case basis by a real satellite constellation because of its internal relative motion; also that the equal edge-lengths of a regular polyhedron represent a maximisation of the minimum inter-vertex distance, which might point to an aspect worth considering in satellite constellation studies. When information was received on a US proposal, by Draim[8], that satellite constellations might advantageously be designed so that the different orbital planes would be parallel to the faces of a regular polyhedron, with the satellite phasing also based on the characteristics of a regular polyhedron, it was felt that this proposal deserved further examination in association with a further study of Critchlow's work.

It was found that most of Draim's suggested constellations required more than one inclination, which would probably be unacceptable in practice; however, one which required only one inclination (Draim's octahedron constellation, with five satellites in each of four planes of 54.736° inclination) was found to be identical to the delta pattern 20/4/2 which the present writer had examined in 1975. From the work on delta patterns it appeared that the optimum inclination for pattern 20/4/2 would be considerably less than 54°, and that some other 20-satellite delta patterns could provide better coverage; it was therefore concluded that Draim's specific proposal did not lead to optimum results. However, on re-examination of Critchlow's work[9] it was realised that the characteristics of regular tesselations (*ie* regular partitions of a plane surface) might give more guidance than those of regular polyhedra (which provide regular partitions of a spherical surface), and a study of this aspect made during 1982 is reported here. This study has (i) identified trends with respect to increases in the number of satellites (T) and the degree of coverage (n) which appear relevant also to regular polyhedra and to practical satellite constellations; (ii) provided a basis for normalising values of $R_{MAX,n}$ and D_{MIN} so as to permit extrapolation of results established previously to higher values of T and n ; and (iii) provided a basis for an examination of a potential combined criterion which demonstrated the relative importance of D_{MIN} , suggesting its use as sole criterion for preliminary studies to establish a short-list of suitable patterns to meet any particular requirement.

To provide a more logical development of the discussion than would a strictly chronological description, this account of these studies begins in section 2 with a discussion of those selection criteria which the writer has found useful in general coverage studies (as opposed to the more detailed criteria which may be developed for analysis of specific satellite system requirements). Section 3 describes the 1982 analysis of tesselations and regular polyhedra, and section 4 includes both the application of this analysis to practical satellite constellations and the results of the 1977 studies of

D_{MIN} . Section 5 covers the 1980 investigations of 18-satellite patterns potentially suitable for GPS, including both the re-examination of 1974-5 computer results and the brief study of characteristics of non-uniform patterns. Finally, the principal conclusions are summarised in section 6.

2 REQUIREMENTS AND SELECTION CRITERIA

2.1 General

The problem with which we are concerned is that of providing, in the most efficient manner, an array of satellites which can between them provide continuous multiple (n-fold) coverage of the entire surface of the Earth. Since, to provide whole-Earth coverage, the satellites must necessarily be in multiple intersecting orbits, the pattern which the satellites form relative to the Earth is constantly changing, and the coverage requirements must be met by all the configurations which the satellite constellation takes up - in other words, we must ensure that the requirements are still met under worst-case conditions. This is, therefore, a more complex problem than that of providing an array of earth-stations able between them to provide continuous multiple sightings of a satellite in any orbit (above a certain altitude) about the Earth, since the earth-stations would form a fixed pattern. Nevertheless, we can obtain some useful insights from examination of this simpler earth-station problem, and of an even simpler problem regarding plane arrays of sensors, as we shall consider later.

2.2 Circumcircle radius and effective horizon

Coverage studies have generally been conducted in terms of the radius from the sub-satellite point to the effective horizon, this radius being measured by the angle it subtends at the centre of the Earth. The 'effective' horizon reflects the particular requirements, depending on satellite altitude and on the minimum acceptable elevation angle from a point on the Earth's surface; for example, for satellites in 12-hour circular orbits to be visible at a minimum elevation angle of 5°, this condition would be met within a radius of 71.2° of a sub-satellite point (from Fig 1 of Ref 1).

Fig 1a represents the instantaneous positions of the sub-satellite points of three out of a constellation of satellites in circular orbits. A circle whose radius represents the effective horizon distance has been drawn (with a solid line) around each sub-satellite point. These circles divide the area covered by this figure into three types of element: within those marked 1, one satellite is visible; within those marked 2, two satellites are visible; while within that marked 0, no satellite is visible. If the radius of the circles were increased to allow for an increased horizon range (*eg* satellites in higher orbits, or lower minimum elevation), the area marked 0 would shrink, as shown in Fig 1b, and full single coverage of this area would eventually be achieved when the three circles all passed through the point + at its centre; this is the centre of the circumcircle (drawn with a broken line) of the three sub-satellite points, and the radii of the three circles would then be equal to this circumcircle radius. Thus the centre of the circumcircle of three adjacent sub-satellite points represents, for that part of the overall pattern, the worst case for meeting the single coverage requirements; and the centre of the largest of such circumcircles is the worst

case for the whole pattern. Considering the variation of the pattern during an orbital period, the largest value of the largest such circumcircle radius (ie $R_{Max,1}$) defines the pattern's single coverage capabilities; it is desirable that this value should be as small as possible.

Fig 1c represents, in similar fashion, the instantaneous positions of four neighbouring sub-satellite points. The point + at the centre of the area within which only one satellite is visible is the centre of the circumcircle of the outer three sub-satellite points, which encloses the fourth sub-satellite point; if the radius of the horizon circles were increased to equal that of the circumcircle, full double coverage of the area would be obtained. In general, the centre of the circumcircle of any three sub-satellite points is the locally critical point for degree of coverage n , where (n - 1) is the number of other sub-satellite points enclosed within the circumcircle.

Fig 1d illustrates the situation when the circumcircle of any three sub-satellite points passes simultaneously through one or more (in this case two) additional sub-satellite points. In Fig 1d, as in Fig 1c, one other sub-satellite point is enclosed within the circumcircle, so that the centre of the circumcircle is again the locally critical point for double coverage. However, under these circumstances it should also be considered a locally critical point for triple and quadruple coverage, since minimal changes in the positions of one or two of the sub-satellite points lying on the circumcircle could leave two or three sub-satellite points, instead of only one, enclosed within the circumcircle. Hence if the circumcircle passes through x sub-satellite points (where x is not less than 3), and encloses y other sub-satellite points, its centre is the locally critical point for degrees of coverage (n) from (y + 1) to (x + y - 2) - though since x will often be equal to 3, these values will often be equal.

The smaller the circumcircle radius, the higher is the minimum elevation angle at which the required number of satellites (at a given orbital altitude) can be seen from any point within the circumcircle. Likewise, the smaller the circumcircle radius the lower is the orbital altitude necessary for the required number of satellites to be visible (above a given minimum elevation angle) from any point within the circumcircle. Thus in general terms it is desirable that the largest value of circumcircle radius ($R_{Max,n}$ or $R_{MAX,n}$) should be as small as possible. However, once the requirements for a particular system have been chosen, and the satellite altitude and minimum elevation angle (determining the maximum circumcircle radius), the required degree of coverage (n) and the number of satellites in the system have all been specified, it might be argued that it is only necessary to confirm that all satellite patterns placed on the short-list for selection meet the stated requirement for maximum circumcircle radius, and that the choice between them should depend not on which of them has the smallest such radius but on some other criterion.

2.3 Inter-satellite distance

Another criterion which has previously been used by the author, with increasing emphasis in successive papers (though still as a criterion additional to the circumcircle radius), is the minimum inter-satellite distance. In the earliest paper[1] it was simply

stated that "The minimum satellite separation ... may be of interest if pairs of satellites are to be used for position-fixing ...", and a similar comment was made in Ref 2. In Ref 3 lists were provided of patterns giving minimum values of $R_{MAX,n}$ for different values of T (from 5 to 15) and of n (from 1 to 4), with the inclination at which this occurred and the value of D_{Min} at this inclination, with the comment that "Apart from considerations of interference, [the value of D_{Min}] is likely to be particularly significant where position determination using more than one satellite is required; no pattern giving a value of D_{Min} less than 3^{o} has been included in the table, and where the value of D_{Min} is small an alternative pattern giving a larger value is listed". Ref 4 said "It is assumed that, as a secondary objective, the minimum separation between any two satellites in the pattern should be as large as possible. The direct importance of this objective may vary according to the system application; in a satellite navigation system, accuracy may well increase as the minimum distance between the satellites providing the fix increases, while in a satellite communications system it may only be necessary that the minimum distance should exceed some fixed value, to ensure that interference between transmissions in the same frequency band is acceptably small. However, it also has some indirect importance in relation to the main objective; the larger the minimum distance between satellites, the more uniform the distribution of satellites over the Earth's surface, and hence the more likely that the pattern will provide relatively favourable values of the maximum distance to the nth nearest sub-satellite point, for all relevant levels of coverage". Ref 4 later noted that "For most purposes it would be unsatisfactory to choose a satellite pattern in which pairs of satellites passed very close to one another; this might cause radio interference, reduce the number of independent observations available from the system, or cause other undesirable effects, even if the possibility of physical collision were discounted"; and, referring to tables presenting, as in Ref 3, values of $R_{MAX,n}$ with associated values of δ_{opt} and D_{Min}, Ref 4 commented that "If it were important, for a particular system, that the minimum satellite separation should be as large as possible, then it would be appropriate to optimise for D_{MIN} rather than for $R_{MAX,n}$, or at least to aim for a compromise between the two".

Ref 5 first presented some results of optimising for D_{MIN}, and showed that the largest values of D_{MIN} were associated with particular sets of delta patterns which had been identified in Ref 4 as being associated with single non-self-crossing repetitive Earth-tracks. It noted that "two types of requirement are likely to be generally applicable to systems requiring continuous multiple whole-Earth coverage. One concerns the level of coverage required (single, double ... n-fold) and the corresponding minimum elevation angle to the nth nearest satellite, and the other the minimum angular separation between adjacent satellites in the pattern, as measured at the centre of the Earth". Hence, over the series of papers, the inter-satellite distance has been treated initially as a feature which might be of interest in some circumstances; later as a secondary objective for optimisation; and most recently as the object of one out of a pair of requirements. Hence, if the circumcircle radius were to be treated only as being subject to an upper limit, rather than as the subject of an optimisation, the inter-satellite distance might be a suitable choice as an alternative subject for

optimisation. However, there are circumstances in which the requirement for the inter-satellite distance itself might only be that it should exceed some specified minimum value.

2.4 The possibility of a combined criterion

Ref 4 suggested the possibility that one might "aim for a compromise between the two". Certainly there are difficulties in having two separate, and sometimes conflicting, criteria for optimisation; later in this Report we shall examine further a possible method of combining the two objectives into one, and the consequences of so doing. However, while it has appeared clear that patterns having a large value of the minimum inter-satellite distance would also provide favourable values of circumcircle radius, the precise nature of the relationship between these criteria for any particular pattern was not obvious; and it was thought that an examination of the simpler earth-station problem, using regular polyhedral patterns, might help to clarify this situation.

3 ANALYSIS OF REGULAR AND SEMI-REGULAR POLYHEDRA AND TESSELATIONS

3.1 General considerations

It seems clear that an ideal solution to the earth-station problem, that of most economically providing an array of stations able to track at all times a satellite in any orbit exceeding a given altitude, would be provided by placing stations at positions corresponding to the vertices of one of the regular polyhedra, if the altitude were such as to make such a number of stations appropriate. However, as is well known, there are only five regular (Platonic) polyhedra, namely the tetrahedron, octahedron, cube, icosahedron and dodecahedron, having respectively 4, 6, 8, 12 and 20 vertices, so the chances of meeting any specific requirements by means of such an ideal solution are limited.

Critchlow[9] has provided a comprehensive review of the regular and semi-regular polyhedra and tesselations, showing that, in addition to the five regular polyhedra, there are 13 semi-regular (Archimedean) polyhedra; of these, two have 12 vertices, four have 24, one has 30, one has 48, four have 60 and one has 120. Thus these add relatively little to the chances of obtaining an ideal solution to the earth-station problem. They share with the regular polyhedra the property of having only a single value of edge-length (or inter-station distance), but whereas the regular polyhedra each have only a single face configuration consisting of a regular polygon (triangular for tetrahedron, octahedron and icosahedron, square for the cube and pentagonal for the dodecahedron), the semi-regular polyhedra each have either two or three different types of regular polygons forming their faces.

However, we may appropriately consider the regular and semi-regular tesselations of a plane as forming extensions of these series of regular and semi-regular polyhedra, since the plane may represent part of the surface of a sphere of infinite radius. Critchlow shows that (using his nomenclature) there are only three regular tesselations (triangular, square and hexagonal), each having a single edge-length, vertex configuration and regular polygonal face shape; eight 'semi-regular' tesselations, each having a single edge-length and vertex configuration but two or three different regular polygonal face

shapes; and 14 'demi-regular' tesselations, each having a single edge-length but two or three different vertex configurations and from two to four different regular polygonal face shapes. With such tesselations one may choose to consider an area containing any arbitrary number of vertices, from zero to infinity.

Whereas we have previously discussed the optimisation problem in terms of 'satellites' or 'earth-stations', these are inappropriate terms to use in relation to a plane surface, so we shall speak instead of arrays of 'sensors' deployed at positions corresponding to the vertices of tesselations. For example, we may imagine an array of sensors deployed on a flat plain to track the movements of animal herds; detection by several sensors simultaneously is necessary for reliable tracking, but individual sensors have a limited radius of sensitivity (or effective horizon distance), and may interfere with one another if sited too close together. Since trade-offs may be possible between sensitivity, interference and number of simultaneous detections necessary, it would be desirable to examine the relationships between these quantities for different types of tesselation; there are thus direct parallels with the earth-station and satellite-constellation problems.

We first consider the three regular tesselations, as shown in Fig 2. The basic dimension for each is the edge-length (or inter-sensor distance) L. Each tesselation may be divided into equal-area cells each containing a single sensor, as shown on the right-hand part of each diagram; their areas correspond to rectangles of sides $L \times \sqrt{3}/2\ L$ for the triangular tesselation, $L \times L$ for the square tesselation, and $3/2\ L \times \sqrt{3}/2\ L$ for the hexagonal tesselation. Hence the average number of sensors per unit area, which we shall denote by S, is $1.15470/L^2$ for the triangular tesselation, $1.00000/L^2$ for the square tesselation, and $0.76980/L^2$ for the hexagonal tesselation; or, for a fixed density of sensors per unit area, the inter-sensor distances L are in the ratio of 1.07457 for the triangular tesselation to 1.00000 for the square tesselation and 0.87738 for the hexagonal tesselation.

When evaluating satellite patterns over a spherical Earth, we are usually comparing patterns containing the same total number of satellites (T), distributed over a fixed area (the spherical surface of the Earth), on the basis of the effective horizon distance ($R_{Max,n}$) at which a given level of coverage (n) can be achieved, and possibly also on the basis of the associated minimum inter-satellite distance D_{Min}; $R_{Max,n}$ should preferably be small, and D_{Min} large. We may apply similar concepts to the tesselations, substituting 'sensors' for 'satellites'; however, since there are no potential variations in the tesselations corresponding to those due to changing satellite phase and orbital inclination, it is sufficient to refer only to values of $R_{MAX,n}$ and D_{MIN}.

For any tesselation T and n will, if large, be closely proportional to the associated surface area. If the values of T, n and the associated surface area are all large and fixed then the value of $R_{MAX,n}$ is also fixed, independent of which of the tesselations is involved, and is proportional to $\sqrt{n}$. On the other hand the value of L (*ie* of D_{MIN}) will depend on which tesselation is involved; the value of D_{MIN} will be largest (*ie* most favourable) for the triangular tesselation and smallest for the hexagonal.

For large values of T and n , circumcircles defining the effective radius of coverage will enclose large numbers of the unit equal-area cells, so that there will be close correspondence between the measured value and the average value for number of sensors enclosed within a circle of given radius, and hence area. However, as the values of T and n become smaller, these values will increasingly tend to vary from the average values common to the three tesselations, and to vary in different ways for the three tesselations, dependent on the detailed geometry of each. The examination of this effect is discussed in the following section.

3.2 Determination of $R_{MAX,n}$ for tesselations

We consider first the triangular tesselation, as shown in Fig 3a. For this case $R_{MAX,1}$ corresponds to the radius of the circumcircle of three adjacent sensors forming one of the basic triangles, ie the circle A; its centre, also marked A, lies on the central vertical line, and its radius may be calculated to be 0.5774L. $R_{MAX,2}$ corresponds to the radius of the circumcircle enclosing one other sensor, ie the circle B, with radius L; this actually passes through a total of six sensors.

To develop a complete list of values of $R_{MAX,n}$ as n is increased, we need (i) to identify all the different circles which pass through three or more sensors; (ii) to find for each circle the number (x) of sensors through which it passes and the number (y) it encloses, thereby obtaining (as in section 2.2) the corresponding value or values of n ; (iii) to calculate the radius of each circle; and then (iv), for each value of n , to find which circle has the largest radius. To ensure that all circles have been identified, it is advisable first to compile a list of all which pass through a pair of adjacent sensors, as in Fig 3a, and then to repeat this process for other pairs of sensors situated at increasing distances apart; one example for another pair of sensors is shown in Fig 3b. Each list may be checked for internal consistency in terms of the increased numbers of sensors lying on or within successive circles of increasing radius, and the lists may then be combined into a single master list arranged in increasing order of radius, the duplications which inevitably occur between different lists providing a second check on consistency. (It may be noted that circles E, G and - are duplicated as between Figs 3a and 3b; the circle identification letters were allocated after compilation of the master list.) Table 1 contains as examples the individual lists corresponding to Figs 3a and 3b, and Table 2 contains the master list for the triangular tesselation; in this a stepped line has been drawn between the values of n to separate the critical case (ie that corresponding to the largest circumcircle radius) for each value of n , lying below and to the left of the line, from non-critical cases lying above and to its right.

It can be seen from Fig 2 that the hexagonal tesselation is identical to the triangular tesselation with every third sensor in each row removed. Each individual list (and the master list) therefore contains the same circle radii as for the triangular tesselation, but with different values of x and y ; since the 'holes' will appear in different places for different alignments of the tesselation, some circles may appear in the lists with more than one pair of values of x and y , while others may not appear at all. The square tesselation, on the other hand, involves a different set of

circle radii. The resulting master lists appear in Table 3 for the square tesselation and Table 4 for the hexagonal tesselation.

In Tables 1 to 4 the circumcircle radii have been expressed as a function of L, whereas to compare them in the manner normally used for satellite constellations they should be expressed as a function of S, the average number of sensors per unit area, which we found to equal $1.15470/L^2$ for the triangular tesselation, $1.00000/L^2$ for the square tesselation, and $0.76980/L^2$ for the hexagonal tesselation. For a circle of radius R enclosing a large number of unit cells of a tesselation we would expect the corresponding degree of coverage n to be equal to $\pi R^2 S$, *ie* we would expect R_n to be equal to $\sqrt{n/\pi S}$. It is of interest to compare the values of $R_{MAX,n}$ found for the three regular tesselations for relatively small values of n with these expected values. A normalised value of $R_{MAX,n}$, which we shall denote by ρ_n, can be obtained by multiplying the values of radius/L in Tables 2 to 4 by $L\sqrt{\pi S/n}$, *ie* by $1.07457\sqrt{\pi/n}$ for the triangular tesselation, by $\sqrt{\pi/n}$ for the square tesselation, and by $0.87738\sqrt{\pi/n}$ for the hexagonal tesselation; values of ρ_n would be expected to approach 1.0 for large values of n. As values of $R_{MAX,n}$, and hence of ρ_n, should preferably be small, the value of $1/\rho_n$ may be regarded as a figure of merit for the tesselation in respect of the actual value of $R_{MAX,n}$ achieved, a value less than 1.0 being inferior to the 'expected' value.

Table 5 lists, for each value of n, the critical values of radius/L for the three regular tesselations as found in Tables 2 to 4, with the corresponding values of ρ_n and $1/\rho_n$. In Fig 4 values of $1 - 1/\rho_n$ for these tesselations have been plotted against n on a semi-logarithmic scale; this suggests that, to a first approximation, values of $1/\rho_n$ for these tesselations approach the value 1.0 exponentially as n increases, according to the relationship $1/\rho_n = 1 - pe^{-qn}$, where $p = 0.16$ and $q = 0.08$. The scatter about the straight line corresponding to this relationship appears random (though in reality all individual values are strictly defined) and is within limits of factors between 3.2 and 1/3.2 on the value of p, *ie* between $p = 0.05$ and 0.512. It may be noted that if we choose, for each value of n from 1 to 16, whichever of the three tesselations provides the largest value of $1/\rho_n$, the resulting values (seven from the triangular, seven from the square and two from the hexagonal tesselations) lie between narrower limits corresponding to $p = 0.05$ and $p = 0.17$, with a likely value of p of about 0.092. (Note that p is equal to the value of $1 - 1/\rho_n$ when $n = 0$.)

We have so far considered only the regular tesselations; however, their very regularity makes them appear remote from the conditions encountered with practical satellite constellations, which have numerous different values of inter-satellite distance from which D_{Min} must be found, and numerous different values of R_n from which the value of $R_{Max,n}$ must emerge for any given value of n. To see how a less regular pattern affects the results obtained, three other tesselations have been examined; they were chosen to show the effects of including differing face shapes, differing vertex configurations and differing edge-lengths. Like the hexagonal tesselation, they are all obtained from the triangular tesselation by omitting certain sensors, so that the same list of calculated values of radius/L may be used.

The first of these, shown in Fig 5a, we shall refer to as 'tri-hex A'; it was listed by Critchlow[9] as semi-regular tesselation No.1, having a single edge-length, a single vertex configuration, and two different (triangular and hexagonal) face shapes. It is obtained from the triangular tesselation by omitting no sensors from one row, alternate sensors from the next, none from the next, and alternate sensors from the following row staggered relative to those in the second row, *ie* omitting one sensor in four overall. The sensor density S is therefore three-quarters of that for the triangular tesselation, *ie* $0.86603/L^2$, and the relative inter-sensor distance is 0.93060.

The second of these other tesselations, shown in Fig 5b, we shall refer to as 'tri-hex B'; it was listed by Critchlow[9] as demi-regular tesselation No.6, having a single edge-length, two different vertex configurations, examples of which are ringed on Fig 5b (one has similar faces opposite, the other similar faces adjacent), and two different face shapes, again triangular and hexagonal. Like tri-hex A it is obtained from the triangular tesselation by omitting alternate sensors from even-numbered rows, but with no staggering between those rows; the sensor density and relative inter-sensor distance are the same as for tri-hex A.

The third such tesselation, which we shall refer to as "the rectangular tesselation", is shown in Fig 5c; it is obtained from the triangular tesselation by omitting alternate rows entirely. It thus has two different edge lengths, L and L' , with $L' = \sqrt{3}\,L$; L , as the smaller value, corresponds to D_{MIN} . The sensor density is half that for the triangular tesselation, *ie* $0.57735/L^2$, and the relative value of L is 0.75984.

As with the hexagonal tesselation, the 'holes' in these tesselations appear in different places for different alignments, so multiple circumcircle lists are required; Table 6, corresponding to part of Table 1, gives as an example the lists for the circumcircles shown in Fig 3b. Such lists are then combined into master lists, as was done in Tables 2 to 4, and from these emerges Table 7, which corresponds to Table 5 for the regular tesselations; the values of radius/L in Table 7 come direct from the master lists, and the values of ρ_n are obtained by multiplying the values of radius/L by $0.93060\sqrt{\pi/n}$ for the tri-hex tesselations and by $0.75984\sqrt{\pi/n}$ for the rectangular tesselation.

The resulting values of $1/\rho_n$ are plotted in Fig 6; for comparison, the lines corresponding to the likely and limiting values for the regular tesselations, as found from Fig 4, are superimposed on this figure. Though the differences are not marked, it appears that the likely values of $1/\rho_n$ for the tri-hex tesselations may be slightly lower than those for the regular tesselations for small values of n (though they would still approach 1.0 for large values of n); if so, this may be associated with the larger size of the unit equal-area cells of the tri-hex constellations, each enclosing three sensors, as shown on the right-hand side of Fig 5a&b. More noticeably, it appears that the likely values of $1/\rho_n$ for the rectangular tesselation may also be lower; this may be associated with the fact that the value of L is now less than the mean inter-sensor distance. In the relationship $1/\rho_n = 1 - pe^{-qn}$, the value $q = 0.08$ still appears appropriate, but the likely value of p for these tesselations appears to be about 0.21, with limiting values of $p = 0.21 \times 2.4$ and $0.21/2.4$, *ie* 0.0875 and 0.504.

A point of interest to note, for the three regular tesselations in Table 5 and the tri-hex tesselations in Table 7, is that when n is 2 the value of $R_{MAX,n}/L$ is 1.0 in each case, *ie* $R_{MAX,2} = L$; this is because, with a single value of edge-length, the $(n = 2)$ circumcircle must have a vertex at its centre, and its radius is therefore equal to the edge-length. Hence $D_{MIN} = R_{MAX,2}$. For the rectangular tesselation, however, with its differing edge-lengths, D_{MIN} is less than $R_{MAX,2}$.

3.3 Determination of $R_{MAX,n}$ for regular polyhedra

Having established some of the trends associated with patterns based on regular tesselations of a plane surface, it is worth considering the regular polyhedra as representing a basis for patterns covering a spherical surface, and hence as an intermediate step between the tesselations and practical constellations of orbiting satellites.

The vertices of the regular polyhedra may be considered as points on a spherical surface at latitudes and longitudes (for one possible orientation) as follows:

Tetrahedron : latitude 35.2644° at longitudes 0° and 180°;
latitude -35.2644° at longitudes 90° and 270°.

Octahedron : latitude 35.2644° at longitudes 0°, 120° and 240°;
latitude -35.2644° at longitudes 60°, 180° and 300°.

Cube : latitudes 35.2644° and -35.2644°
at longitudes 0°, 90°, 180° and 270°.

Icosahedron : latitudes 52.6226° and -10.8123° at longitudes 0°, 120° and 240°;
latitudes 10.8123° and -52.6226° at longitudes 60°, 180° and 300°.

Dodecahedron : latitudes 52.6226° and 10.8123° at longitudes 0°, 72°, 144°, 216° and 288°; latitudes -10.8123° and -52.6226° at longitudes 36°, 108°, 180°, 252° and 324°.

From these coordinates one may (using standard formulae of spherical trigonometry) calculate circumcircle radii, in terms of the angle subtended at the centre of the Earth, and for each circle find the corresponding values of x and y, and hence the relevant values of n. These are listed in Table 8; brackets have been placed round non-critical values of n. As for the regular tesselations, L (or D_{MIN}) is equal to the second radius listed in each case.

Values of $R_{MAX,n}$ extracted from Table 8 are listed in Table 9 for all values of n relevant to each of the regular polyhedra. The procedure for deriving values of σ_n is a little different from the case of the tesselations. Here we have a fixed area, that of the spherical surface $(4\pi r^2)$, associated with the total number (T) of vertices of the polyhedron, so that $S = T/4\pi r^2$. Since $\sigma_n = \sqrt{\pi S/n} \times R_{MAX,n}$, values of σ_n for the different polyhedra are obtained by multiplying $R_{MAX,n}$ by $\sqrt{T}/2r\sqrt{n}$, where $2r$ corresponds to $360^\circ/\pi$, *ie* by

$\frac{\sqrt{}}{180} \times \frac{1}{\sqrt{n}}$ for the tetrahedron,

$\frac{\sqrt{6}}{360} \times \frac{1}{\sqrt{n}}$ for the octahedron,

$\frac{\sqrt{2}}{180} \times \frac{1}{\sqrt{n}}$ for the cube,

$\frac{\sqrt{3}}{180} \times \frac{1}{\sqrt{n}}$ for the icosahedron and

$\frac{\sqrt{5}}{180} \times \frac{1}{\sqrt{n}}$ for the dodecahedron.

The resulting values of ρ_n and $1/\rho_n$ are listed in Table 9, and values of $1/\rho_n$ are plotted against n in Fig 7a, with the straight lines from Fig 4 corresponding to likely and limiting values for regular tesselations superimposed for comparison. While all the calculated values of $1/\rho_n$ are plotted on Fig 7a, we are really only interested in those derived from values of $R_{MAX,n}$ less than 90°, since larger values give no visibility round the spherical Earth; these lower values are therefore distinguished by solid symbols. It appears from Fig 7a that the likely values of $1/\rho_n$ for regular polyhedra may well be following a similar trend to that for regular tesselations (though at slightly lower values) while $R_{MAX,n}$ is less than 90°, but that as $R_{MAX,n}$ exceeds 90° and approaches 180° the values of $1/\rho_n$ tend to fall. While the usual scatter of values makes it difficult to identify such trends with confidence, it appears that the relationship $1/\rho_n = 1 - pe^{-qn}$ may again be appropriate when $R_{MAX,n}$ is less than 90°, with q again equal to 0.08 and the likely value of p equal to 0.21, with limiting values of $p = 0.21 \times 1.8$ and $0.21/1.8$.

3.4 Determination of D_{MIN} for tesselations and polyhedra

We have already noted values of L, which also represent the values of D_{MIN}, for the various tesselations and the regular polyhedra; L is proportional to $1/\sqrt{S}$, and relative values are, for the tesselations, 1.07457 for the triangular, 1.00000 for the square, 0.87738 for the hexagonal, 0.93060 for tri-hex A and B and 0.75984 for the rectangular; and for the regular polyhedra, 1.07796 for the tetrahedron, 1.08540 for the octahedron, 0.98216 for the cube, 1.08191 for the icosahedron and 0.92060 for the dodecahedron. Thus the four triangular-faced figures all provide values approximating to 1.1, compared with 1.0 for the two square-faced figures, 0.92 for the pentagonal-faced dodecahedron and 0.88 for the hexagonal tesselation. The rectangular tesselation, with two different edge-lengths, gives a considerably lower value at 0.76, while tri-hex A and B fall between the levels for triangles and hexagons.

It appears appropriate to normalise the values of D_{MIN}, as was done for $R_{MAX,n}$, so as to give an expected value of 1.0 for a large area of an optimum tesselation, and smaller values for less satisfactory values of D_{MIN}. Since D_{MIN} should preferably be large, and the triangular tesselation is the one giving the largest value, normalised

values of D_{MIN} (which we shall call λ) may be obtained simply by dividing the relative values by 1.07457. Resulting values of λ are:

triangular tesselation 1.0000, tetrahedron 1.0032, octahedron 1.0101, icosahedron 1.0068;

square tesselation 0.9306, cube 0.9140;

dodecahedron 0.8567;

hexagonal tesselation 0.8165;

tri-hex A and B 0.8660; and

rectangular tesselation 0.7071.

The fact that the triangular-faced polyhedra have values of λ slightly exceeding 1.0 may detract from the neatness of this approach, but is irrelevant to our ultimate objective of deriving values of $1/\sigma_n$ and λ for practical satellite constellations.

Values of λ may be obtained directly from values of D_{MIN} which have been measured on a spherical surface in terms of degrees subtended at the centre of the sphere by multiplying by $\sqrt{\pi T\sqrt{3}/2}/360^\circ = \sqrt{T}/218.254$.

3.5 A combined criterion

In the light of our consideration so far of the application of the separate criteria $R_{MAX,n}$ and D_{MIN}, and the corresponding normalised criteria $1/\sigma_n$ and λ, it is worth examining the possibility of a combined criterion to meet the objective suggested in section 2.4.

An obvious candidate for consideration is the product of the two normalised criteria $1/\sigma_n$ and λ; since each approaches the value 1.0 under ideal conditions, while otherwise giving smaller values, their product will do the same. λ/σ_n is proportional to $D_{MIN}/R_{MAX,n}$; this is non-dimensional, since both D_{MIN} and $R_{MAX,n}$ are distances measured on the surface of a sphere. We shall denote the product λ/σ_n by ε_n; since $1/\sigma_n = 360^\circ \times \sqrt{n/T}/\pi R_{MAX,n}$, and $\lambda = D_{MIN} \times \sqrt{\pi T\sqrt{3}/2}/360^\circ$, we have

$$\varepsilon_n = \left(\frac{D_{MIN}}{R_{MAX,n}}\right)\sqrt{\frac{n\sqrt{3}}{2\pi}}$$

$$= 0.52504\sqrt{n}\,\frac{D_{MIN}}{R_{MAX,n}} \quad ,$$

and we shall test the use of this prospective criterion when we come to examine practical satellite constellations. For the tesselations and regular polyhedra, we need merely note that combining $1/\sigma_n$ and λ in this manner serves to distinguish between the three regular tesselations, giving the advantage to the triangular tesselation, and that it likewise gives the advantage to the three triangular-faced regular polyhedra over the cube and the dodecahedron.

4 APPLICATION OF ANALYSIS TO DELTA PATTERNS

4.1 Derivation of $R_{MAX,n}$ and D_{Min}

In Ref 3 the author listed satellite patterns, containing a total number of satellites (T) between 5 and 15, which for each value of T appeared most economically to provide single, double, triple or quadruple coverage of the whole surface of the Earth. These patterns all belonged to a class of pattern which the author had previously[1] described as 'delta patterns' (and which have since been referred to elsewhere[10] as 'Walker constellations'). As noted in section 1, a delta pattern consists of equal numbers of evenly-spaced satellites in each of P evenly-spaced and equally-staggered planes, all having the same inclination i to a reference plane (usually, but not necessarily, the equator). It may be identified by the three-integer code reference T/P/F, where F (measured in units of $360^\circ/T$) is a measure of the relative phasing between satellites in adjacent planes; specifically, when a satellite in one plane is at its ascending node, a satellite in the adjacent plane having a more easterly ascending node is $(360\ F/T)^\circ$ past its ascending node.

Table 10 lists, for each value of T, the delta pattern giving the smallest value of $R_{MAX,n}$ (for values of n from 1 to 4), as quoted in Ref 3, together with this value of $R_{MAX,n}$, the inclination i_{opt} at which it occurred, and the corresponding value of D_{Min}. From these values the normalised criteria σ_n, $1/\sigma_n$, λ and ϵ_n (defined as for the regular polyhedra) have been calculated, and are also listed.

It should be noted that, for T = 10, the pattern 10/10/7 actually gives a slightly smaller value of $R_{MAX,1}$ (51.5° at a i_{opt} of 47.9°, with $D_{Min} = 0^\circ$) than the pattern 10/5/2 listed here. Pattern 10/10/7 has been listed by Mozhaev[11] and Ballard[12], but the present writer chose to exclude from his listings any pattern giving a value of D_{Min} less than 3°, as unlikely to be acceptable for a practical satellite system; 10/10/7 is a pattern for which P and F - T/P are both even numbers, which identifies it (see section 3.5 of Ref 4) as one for which $D_{Min} = 0^\circ$ at all inclinations, and so pattern 10/5/2 appears preferable. Pattern 10/10/7 would have zero values of λ and ϵ_n.

Table 10 also includes five further patterns, having values of T between 16 and 24, which were listed in Ref 4 as giving optimum values of $R_{MAX,n}$ for values of n between 4 and 7.

Fig 7b is a semi-log plot against n of the values of $1/\sigma_n$ corresponding to these smallest values of $R_{MAX,n}$, again with the lines from Fig 4 (corresponding to likely and limiting values for regular tesselations) superimposed on it. It appears that the value of q = 0.08 is again appropriate, with limiting values of p of about 0.20 and 0.34, and a likely value of p of about 0.26. Figs 7c and 7d will be discussed in the following section.

4.2 Derivation of D_{MIN} and $R_{Max,n}$

Prior to 1977 the author did not attempt to determine values of D_{MIN} for delta patterns, concentrating instead on determination of values of $R_{MAX,n}$ and the associated

values of D_{Min} . In 1977, however, following up an observation noted in Ref 4 that two series of patterns listed in its Table 1 appeared to give the largest values of D_{Min} for values of T above and below 10 respectively, values of D_{MIN} and the inclinations ($i_{opt,D}$) at which they occurred were determined (using an abbreviated version of the program COCO) for four such series of patterns, for values of T up to 25, and a plot of D_{MIN} against T was provided in Fig 3 of a brief paper[5] presented in 1978. This is reproduced as Fig 8 of the present Report, while in Fig 9 values of $i_{opt,D}$ are plotted against T for the same four series of patterns. These patterns, identified by their code reference T/P/F, are listed in Table 11 together with the corresponding values of D_{MIN}, $i_{opt,D}$ and λ .

The four series of patterns are those which would follow single non-self-crossing Earth-tracks if used at periods of 12 h, 16 h, 18 h or 19.2 h, *ie* they would complete L orbits in M days, where L:M equals 2:1, 3:2, 4:3 or 5:4. It was shown in Ref 4 that non-self-crossing Earth-tracks, corresponding to a well-spaced distribution of satellites, are obtained when L - M = 1, and that this favourable distribution is retained independent of the period at which the pattern is actually used. The delta patterns associated with these values of L:M are identified by having P equal to the value of T divided by the highest common factor of T and M , and F equal to T(kP - L)/PM , where k takes whatever integer value is necessary to make F an integer in the range 0 to P - 1.

The largest value of D_{MIN} is given by the 2:1 series for values of T from 5 to 9, by the 3:2 series from 10 to 24, and by the 4:3 series from 25 upwards; the second-largest value is given by the 3:2 series for values of T below 10 and above 24, by the 2:1 series from 10 to 15 and by the 4:3 series from 16 to 24. Fig 8 suggests that the 5:4 series would become relevant when T reached values in the upper twenties or lower thirties. These four series of patterns generally provide the largest values of D_{MIN} for all the patterns having a particular value of T ; for example, a check of all delta patterns having T = 13 shows that, while these four have values of D_{MIN} of 44.1°, 47.3°, 41.7° and 35.6°, the pattern in the 6:5 series has a value of 31.7° and the remainder all have values below 30°. For small values of T , some patterns reach their largest value of D_{MIN} at zero inclination (at which $R_{Max,n} = 90°$); these values all lie on the broken line on the left side of Fig 8. Otherwise, cross-reference to Fig 9 shows that the largest values of D_{MIN} occur at inclinations between 51° and 66°. Reference to Table 10 shows that there is not the same regular pattern to the occurrence of minimum values of $R_{MAX,n}$, though about 80% of the values of i_{opt} listed fall within the same range of inclinations.

As an example of the conditions under which D_{MIN} occurs for the patterns giving non-self-crossing Earth-tracks, Fig 10 shows pattern 13/13/5 at the inclination of 57.6° corresponding to $i_{opt,D}$ and at phase ε = 1.0; under these conditions the distances between satellites CH and LN are both equal to D_{MIN} . If i were increased then D_{Min} (associated with CH) would be less, while if i were reduced then D_{Min} (associated with LN) would be less. For other such patterns D_{MIN} may occur for both pairs when ε = 0 or for one pair when ε = 0 and for the other when ε = 1.0; but in all such cases, one pair is symmetrically placed near the closed end of a loop and the other near the open end of a loop.

The 1977 computer runs to determine values of D_{MIN} and $\delta_{opt,D}$ were not extended to determine corresponding values of $R_{Max,n}$. However, in many cases it has been possible to refer back to the printouts from the runs of the program COCO which determined values of $R_{MAX,n}$ for patterns with T between 5 and 15 in 1971-2, and those for some patterns with T between 16 and 25 in 1974-5, and by interpolation obtain a good approximation to the values of $R_{Max,n}$ corresponding to inclination $\delta_{opt,D}$. This has made it possible to estimate values of ε_n, $1/\varepsilon_n$ and ε_n, as well as λ, corresponding to that inclination. Values are listed in Table 12 for the patterns providing the largest values of D_{MIN} for each value of T, and in Table 13 for those providing the second-largest values.

While the printouts were being examined and values of ε_n calculated at δ_{opt} and $\delta_{opt,D}$, values were also calculated at other inclinations in order to find the maximum values of ε_n and the inclinations at which they occurred. It was found that (with one exception) the maximum value of ε_n always occurred at $\delta_{opt,D}$. This is because D_{Min} always falls off much more rapidly as δ is either increased or decreased from the peak at $\delta_{opt,D}$ than $R_{Max,n}$ increases as δ is either increased or decreased from δ_{opt} (as may be seen, for example, from Figs 6 and 7 of Ref 2); the value of ε_n is thus much more sensitive to D_{Min} than to $R_{Max,n}$. The single exception was pattern 5/5/1, which lies on the broken line in Fig 8. For this pattern D_{MIN} occurs at zero inclination and the value of D_{Min} decreases only slowly as δ is increased; the maximum value of ε_n therefore occurs at δ_{opt}, as shown in Table 10.

The values of D_{MIN} in Fig 8, excluding those lying on the broken line, are replotted in Fig 11 in the form of a log-log plot of λ against T (with expanded λ scale). This shows that, as T is increased, values of λ corresponding to each of the $(L - M = 1)$ series tend to rise to a peak and then fall away again, crossing as they do so the rising values for each of the subsequent series as these in turn approach their own peaks. A line representing the envelope of the peaks and another representing the lower envelope of the intersections of the curves representing consecutive series, corresponding to the broken lines in Fig 11, indicate the upper and lower limits of the largest values of λ for a given value of T, and over the range of values of T for which results are available it appears that these can be adequately represented on this log-log plot by the straight lines corresponding to $\lambda = 1.01\ T^{-0.1}$ and $\lambda = 0.96\ T^{-0.1}$, with a likely value between these limits represented by the straight line $\lambda = 0.99\ T^{-0.1}$.

For the delta patterns from the $(L - M = 1)$ series giving the largest values of D_{MIN} (and hence of λ) for each value of T, the values of $1/\varepsilon_n$ at $\delta_{opt,D}$ are plotted against n in Fig 7c; for those patterns giving the second-largest values of D_{MIN}, values of $1/\varepsilon_n$ are plotted in Fig 7d. As in Fig 7b it appears that, over the limited range of values of n for which results are available, the value of $q = 0.08$ remains acceptable; for Fig 7c it appears that the likely value of p is about 0.32, with limits of $0.32/1.33 = 0.24$ and $0.32 \times 1.33 = 0.43$, while for Fig 7d the likely value is a little higher and the limits somewhat wider. Thus optimising for D_{MIN} rather than for $R_{MAX,n}$ appears to increase the value of p such that the likely value approaches what was the less satisfactory of the limiting values for $R_{MAX,n}$, though the corresponding values of [illegible] are naturally much improved.

4.3 The combined criterion ε_n

Values of ε_n at the inclination δ_{opt} have been listed in Table 10, and values at $\delta_{opt,D}$ in Tables 12 and 13 for the relevant patterns. The overall average of the values in Table 12 is 0.566, of those in Table 13 is 0.529, and of those in Table 10 is 0.353. It has already been noted that it was found that, in all cases where $\delta_{opt,D}$ occurred at an inclination acceptable for whole-Earth coverage and not at 0°, the maximum value of ε_n occurred at $\delta_{opt,D}$.

When it was decided to test ε_n as a combined criterion for use with practical satellite patterns, it was thought that it might point to some compromise choice as between those patterns which gave the best values of $R_{MAX,n}$ and those which gave the best values of D_{MIN}, or between the inclinations δ_{opt} and $\delta_{opt,D}$ for a single pattern. Instead the test has shown that there is no such compromise; the choice of pattern, and of inclination for that pattern, is so much more sensitive to D_{MIN} than to $R_{MAX,n}$ that, if it is accepted that D_{MIN} has any relevance to the choice to be made, it almost inevitably becomes the dominant factor in that choice. In that respect, the exercise may be considered to have failed; however, the information it has provided regarding the importance of D_{MIN} is of considerable significance. D_{MIN} is very much simpler to calculate than $R_{MAX,n}$, and if it is possible to use it as the sole criterion during the preliminary screening of satellite patterns for a particular application then much time and effort can be saved.

While these results have suggested that D_{MIN} may prove a more generally useful criterion than $R_{MAX,n}$, it was felt worthwhile to examine separately the values of λ, $1/\rho_n$ and ε_n for those delta patterns giving both the largest and the second-largest values of D_{MIN} for each value of T, as has been done in Tables 12 and 13. One reason for doing so is that, near the cross-over between successive $(L - M = 1)$ series, the values of λ will be very similar and so the values of $1/\rho_n$ may determine which pattern has the larger value of ε_n. Another reason is that the advantages of a particular value of δ or P may become a factor in an otherwise closely-balanced choice; values of $\delta_{opt,D}$ differ significantly between the two tables (as shown also by Fig 9), and for most values of T divisible by 2 or 3 the value of P differs between the patterns in these two tables.

Comparing results for similar values of T and n, it is noted that when $T = 24$ the values of D_{MIN} and λ for the patterns in Tables 12 and 13 are virtually identical, though those for 24/12/9 are actually marginally greater than those for 24/8/4. Their overall similarity is emphasised by the fact that the values of $1/\rho_n$, and hence of ε_n, are greater for 24/12/9 when $n = 1$, 2 or 5, but are greater for 24/8/4 when $n = 3$, 4, 6 or 7. Elsewhere in the tables there are only two cases ($T = 11$, $n = 2$ and $T = 12$, $n = 1$) where a larger value of $1/\rho_n$ results in the value of ε_n being greater in Table 13, and six cases ($T = 7$, $n = 2$; $T = 9$, $n = 3$; $T = 12$, $n = 2$ and 3; $T = 13$, $n = 2$; and $T = 14$, $n = 2$) where the value of $1/\rho_n$ is larger in Table 13, but not sufficiently so to outweigh the larger value of λ in Table 12; in most cases Table 12 contains the larger values of $1/\rho_n$ as well as of λ. We would therefore expect that the pattern in the series giving the largest value of D_{MIN} should be given first consideration, though the pattern

giving the second-largest value might be a suitable choice if there were other reasons for preferring it.

4.4 Discussion

Reviewing the material presented in the preceding sections, in conjunction with that previously presented in Ref 4, suggests the following overall picture of the provision of multiple whole-Earth coverage by means of constellations of high-altitude circular-orbit satellites forming delta patterns.

For any given value of T, the total number of satellites in the pattern, there will be a substantial number of different delta patterns available for consideration; this number is equal to the sum of all the factors of T, including 1 and T. A proportion of these patterns will give values of $R_{MAX,n}$ which may be considered 'good', while a further proportion will give values which may be considered 'poor'; the methods described in section 3 of Ref 4 will identify some of those patterns giving 'poor' values of $R_{MAX,n}$ and/or of D_{MIN}. Among those giving 'good' values of $R_{MAX,n}$, a similar situation is likely to exist to that illustrated in Fig 4 for the regular tesselations, in Fig 6 for the other tesselations and in Fig 7a for the regular polyhedra; while all remain within a band of values which may be considered 'good', there is an irregular variation with the value of n of their relative order of merit, determining which may be considered 'best'. The particular pattern giving the smallest value of $R_{MAX,n}$ for any particular values of T and n can be found through a detailed investigation, but is otherwise unpredictable; while the 'best' values of $R_{MAX,n}$ fall within a more narrowly defined band than the 'good' values.

Turning temporarily from $R_{MAX,n}$ to D_{MIN}, it was shown in Ref 5 (and in Fig 8 of the present Report) that the patterns providing the largest values of D_{MIN} were those which could produce single non-self-crossing Earth-tracks, occurring in series for which L:M is such that $L - M = 1$. Patterns with these characteristics usually avoid the adverse features which lead to a placing in the 'poor' category for $R_{MAX,n}$, and instead are to be found in the 'good' category, with a fair chance of appearing as 'best' at any particular value of n. Since these patterns are readily identifiable by means of formulae developed in Ref 4 (and reproduced in the following section), they provide a convenient starting-point for any coverage study; moreover, we have already shown that they provide the largest values of our test criterion ε_n.

While these conclusions regarding the desirability of identifying those patterns providing the largest values of D_{MIN} (or λ) have been developed specifically through examination of the characteristics of delta patterns, it might be expected that they would have some relevance also to other types of pattern which do not share all the characteristics of delta patterns.

4.5 Predictions

The results which have been discussed in the preceding sections provide new means for predicting the values of $R_{MAX,n}$, or of D_{MIN} and the associated value of $R_{Max,n}$, which might be available for values of T and n greater than those which have already

been explored. For a modest extrapolation, and with somewhat less confidence for a larger extrapolation, we may use the predictions that:

$$R_{MAX,n} \text{ (at } \delta_{opt}) = \frac{360}{\pi}\sqrt{\frac{n}{T}}\,\sigma_n \text{ degrees,}$$

where $1/\sigma_n = 1 - pe^{-0.08n}$ and p lies between limiting values of 0.20 and 0.34, with an expected value of 0.26; hence

$$T = n\left(\frac{360}{\pi}\right)^2 \frac{\sigma_n^2}{R_{MAX,n}^2} .$$

Also

$$D_{MIN} \text{ (at } \delta_{opt,D}) = \frac{218.254\lambda}{\sqrt{T}} \text{ degrees,}$$

where λ lies between limits of $1.01\ T^{-0.1}$ and $0.96\ T^{-0.1}$, with an expected value of $0.99\ T^{-0.1}$. $R_{Max,n}$ (at $\delta_{opt,D}$) is given by the same formulae as $R_{MAX,n}$, but with p lying between limiting values of 0.24 and 0.43, with an expected value of 0.32.

For convenience, values of $1/\sigma_n$ for the six relevant values of p are presented in Table 14, and values of σ_n^2 in Table 15, for values of n from 1 to 10; also the three values of D_{MIN} are presented in Table 16 for values of T from 26 to 40.

No means are available of predicting either the value of D_{Min} associated with the value of $R_{MAX,n}$ at δ_{opt}, or the particular pattern which would provide that smallest value of $R_{MAX,n}$. It can be predicted that the largest value of D_{MIN} will be provided by a pattern in one of the (L - M = 1) series (identified by L:M), and a very rough extrapolation of Fig 11 suggests that from T = 25 to about 30 it would be from the 4:3 series (or perhaps the 3:2 series); from T = about 30 to about 36, from the 4:3 series (or perhaps the 5:4 series); from T = about 36 to about 42, from the 5:4 series (or perhaps the 4:3 series); and from T = about 42 to about 48, the 5:4 series (or perhaps the 6:5 series). The specific pattern T/P/F which is the member of each series for a particular value of T may be determined from the following formulae, developed in Ref 4: P is equal to T divided by the highest common factor of T and M, and F is equal to $T(kP - L)/PM$, where k takes whatever integer value is necessary to make F an integer in the range from 0 to $P - 1$. The patterns forming the 3:2 series, the 4:3 series, the 5:4 series and the 6:5 series for values of T from 26 to 40 are listed in Table 17; for values of T below 26 they were listed in Table 1 of Ref 4 (and, for the first three of these series, in Table 11 of the present Report).

It should be particularly noted that $\delta_{opt,D}$ is the inclination at which the value of D_{MIN} is largest, but that varying the inclination is likely to reveal a smaller value of $R_{Max,n}$. Thus if the pattern which provides the largest value of D_{MIN} at a particular value of T does not meet the coverage requirements at $\delta_{opt,D}$ because it has too

large a value of $R_{Max,n}$ at that inclination, it is still worth finding the value of $R_{MAX,n}$ for that pattern at i_{opt} to see if the requirements can then be met, even though the value of D_{Min} is reduced. For some values of T and n the same pattern provides both the largest value of D_{MIN} at $i_{opt,D}$ and the smallest value of $R_{MAX,n}$ at i_{opt}, as shown by comparison of Tables 10 and 12.

7.6 Examples

To illustrate the use of these prediction methods, we consider some examples of the sort of problem to which they may be applied.

(i) For constellations of satellites in 12-hour circular orbits, with a minimum working elevation angle at the Earth's surface of 5^o (*ie* $R_{Max,n} \leq 71.2^o$), what are the numbers of satellites likely to be necessary to provide continuous multiple whole-Earth coverage to the following standards: (a) four-fold, (b) six-fold and (c) eight-fold continuous coverage?

Using values of c_n^2 from Table 15 for n = 4, 6 and 8, we obtain the following values of T :

(a) for n = 4, T = 14.18, 15.75, 18.24, 15.20, 17.58 and 21.90;

(b) for n = 6, T = 20.25, 22.07, 24.93, 21.43, 24.17, 28.86; and

(c) for n = 8, T = 25.90, 27.83, 30.77, 27.17, 29.98, 34.65.

We may interpret these as meaning that, if we are primarily concerned to provide the specified coverage with the minimum number of satellites and are not concerned if the value of D_{Min} is small, we are likely to be able to meet this objective:

(a) for four-fold coverage, with between 15 and 18 satellites, with 16 as the most likely number required;

(b) for six-fold coverage, with between 21 and 24 satellites, with 22 as the most likely number required; and

(c) for eight-fold coverage, with between 26 and 30 satellites, with 28 as the most likely number required.

(In practice, Table 10 shows that 15 satellites at i_{opt} just meet the requirement for four-fold coverage, and that 24 satellites meet the requirement for six-fold coverage with a substantial margin, suggesting that a smaller number would be adequate.)

If, on the other hand, we are concerned that while meeting the coverage requirement we should also have as large as possible a value of D_{MIN}, we are likely to be able to meet this objective:

(a) for four-fold coverage, with between 16 and 21 satellites, with 18 as the most likely number required;

(b) for six-fold coverage, with between 22 and 28 satellites, with 24 as the most likely number required; and

(c) for eight-fold coverage, with between 28 and 34 satellites, with 30 as the most likely number required.

(In practice, Tables 12 and 13 suggest that 16 satellites at $\delta_{opt,D}$ might just meet the requirement for four-fold coverage, and 24 satellites that for six-fold coverage.)

(ii) If we are interested in eight-fold coverage with a large value of D_{MIN}, (a) what values of D_{MIN} are likely to be obtainable and (b) what appear to be the most promising patterns for initial investigation, preferably avoiding patterns having a large value of P ?

(a) From Table 16, the predicted largest value of D_{MIN} for 30 satellites is 28.1°, the upper limit associated with 28 satellites is 29.9° and the lower limit associated with 34 satellites is 25.3°. Somewhat smaller values would result if we used the pattern giving the second-largest or third-largest value, or used an inclination other than $\delta_{opt,D}$.

(b) The most likely pattern to provide the required conditions is the 30-satellite pattern in the 4:3 series; from Table 17 this is pattern 30/10/6. The next most likely patterns are 30/15/5 and 30/15/12. However, considering the preference for relatively few planes (small value of P), it would be worth investigating 28/7/2 and 30/6/0; or if none of these proved satisfactory, 32/8/3 might be suitable.

(iii) What is the likely value of $R_{MAX,8}$ for 28 satellites?

Using values of $1/\rho_n$ for $n = 8$ from Table 14, the likely value (at δ_{opt}) is 71.0°, with maximum and minimum values of 74.6° and 68.5°. The likely value of $R_{Max,8}$ at $\delta_{opt,D}$ is 73.7°, with maximum and minimum values of 79.2° and 70.1°.

5 USE OF D_{MIN} (OR λ) AS SOLE CRITERION IN A PRELIMINARY STUDY OF NON-UNIFORM ORBITAL PATTERNS

5.1 Background

The particular numerical prediction methods discussed in sections 4.3 and 4.4 were derived only for delta patterns. However, the conclusions developed in sections 4.3 and 4.4 regarding the desirability of identifying those patterns providing the largest values of D_{MIN} (or λ) might be expected to have somewhat wider applicability, and the simplicity of calculating inter-satellite distances makes this appear a suitable criterion for use in preliminary studies, including drawing up short-lists of patterns for subsequent detailed examination against the particular requirements and criteria developed for the system under consideration. D_{MIN} provides a fully adequate comparison between patterns containing similar numbers of satellites, but λ provides a better guide to the standards being achieved, in comparison with the best which might be expected, when different numbers of satellites are involved.

D_{MIN} was of necessity used as the sole criterion in the brief study[7] of non-uniform patterns, and their comparison with 18-satellite delta patterns. This study was occasioned by proposed changes to plans for the GPS satellite navigation system; the writer did not have access to a computer program providing values of the criteria (GDOP and PDOP) normally used for that system, and while it might have been desirable to make use of the full or shortened version of the RAE program COCO, initially developed in 1971 and used until 1976 to calculate the values of $R_{MAX,n}$ initially published in Refs 3

and 4, it was not feasible in the short time then available to adapt this program for analysis of non-uniform patterns (and it would also, with such patterns, have required substantially more computer time). However, the small portion of the program which was used to calculate values of D_{MIN} could be adapted relatively quickly, and so was used in this study; it provides a good example of what may be achieved using D_{MIN} as sole criterion.

Appendix A of Ref 4 discussed the application of the delta pattern analysis to satellite navigation systems such as GPS; showed how, among 24-satellite three-plane patterns, the pattern 24/3/2 appeared preferable to the pattern 24/3/1 which seemed from one account to have been selected (though it was subsequently confirmed that 24/3/2 was indeed the chosen pattern); and, considering partial patterns of 18 instead of 24 satellites, indicated that 18/3/0 and 18/6/2 appeared to be the best three-plane and six-plane 18-satellite delta patterns respectively, with 18/6/2 probably superior.

In 1980 it became known that it was intended to reduce the size of the initial operational GPS constellation from 24 satellites to 18, using 12-hour orbits of 55° inclination, but that it was proposed to retain the option to build up later to the originally planned number of 24 satellites. It was possible that, in addition to the 18 active satellites in orbit, three further satellites might be placed in orbit as inactive spares. It would therefore be desirable to identify patterns which could meet the requirements using only 18 satellites, could be expanded to include 24 satellites, and could accommodate 21 satellites in a suitable manner.

The printouts from the runs of the computer program COCO covering 18-satellite delta patterns which had been made in late 1974 and early 1975 were re-examined[6] for further information relevant to the choice of a system to operate at 55° inclination. In 12-hour orbits the value of $R_{Max,n}$ corresponding to zero elevation is 76.1°, while that corresponding to 5° elevation is 71.2°. For GPS four well-spaced satellites must be visible above 5° elevation at all times, so in drawing up a short-list of potentially suitable patterns it was considered essential to have a value of $R_{Max,4}$ not exceeding 71.2°, and the following arbitrary limits were also set: $R_{Max,1}$ not exceeding 50°, $R_{Max,5}$ not exceeding 85°, and D_{Min} not less than 10°. Seven 18-satellite patterns were found to meet all these criteria at 55° inclination, as shown below:

Pattern	$R_{Max,1}$	$R_{Max,4}$	$R_{Max,5}$	$R_{Max,6}$	D_{Min}
18/3/0	44.8°	65.8°	81.9°	90.0°	20.8°
18/6/2	39.7°	66.8°	76.4°	86.7°	33.3°
18/9/2	42.9°	68.3°	83.8°	87.6°	20.8°
18/9/6	44.8°	70.8°	76.3°	83.6°	34.9°
18/18/2	44.4°	67.8°	76.5°	82.4°	21.3°
18/18/14	40.7°	70.1°	75.0°	80.4°	21.3°
18/18/16	47.8°	67.1°	75.5°	82.8°	28.2°

It was noted that 18/18/4 and 18/18/16 both have values of $R_{Max,5}$ less than 76.1°, showing that with these patterns there would never be less than five satellites above zero elevation, while 18/6/2, 18/9/6 and 18/18/2 have values only slightly greater than 76.1°, showing that any disappearances of a fifth satellite would be rare and brief. Patterns 18/9/6, 18/6/2 and 18/18/16 have the largest values of D_{Min}. However, of the seven patterns only 18/3/0 and 18/6/2 could be expanded to 24-satellite delta patterns; 18/3/0 could also be expanded to a 21-satellite delta pattern, whereas three spares added to the six-plane pattern 18/6/2 could be placed only in alternate planes.

A fuller comparison of the possible expansions of these two patterns, based on the 1974-5 computer runs, is as follows:

Pattern	$R_{Max,1}$	$R_{Max,4}$	$R_{Max,5}$	$R_{Max,6}$	$R_{Max,7}$	D_{Min}	λ
18/3/0	44.8°	65.8°	81.9°	90.0°	90.0°	20.8°	0.404
21/3/2	40.4°	59.0°	76.9°	77.5°	90.0°	14.8°	0.311
24/3/2	38.1°	55.4°	68.2°	69.1°	85.2°	10.8°	0.242
18/6/2	39.7°	66.8°	76.4°	86.7°	90.0°	33.3°	0.647
24/6/1	38.7°	57.6°	69.5°	70.0°	74.5°	20.8°	0.467

This shows that the value of $R_{Max,5}$ for 18/6/2 is very similar to the values of $R_{Max,5}$ and $R_{Max,6}$ for 21/3/2; that both 24/3/2 and 24/6/1 would always have at least six satellites above 5° elevation, but that 24/6/1 would always have at least seven satellites above zero elevation, whereas 24/3/2 would not; and that 24/6/1 has a considerably better value of D_{Min} (and λ) than 24/3/2. Despite the advantage of the three-plane series in terms of the convenient positioning of spares, the six-plane series appears preferable overall.

Fig 12 illustrates the satellite distributions in some of these patterns. Fig 12a shows pattern 24/3/2 (taking account of both cross and circle symbols; the reason for using two symbols will be explained later), while Fig 12b-d shows patterns 18/3/0, 18/6/2 and 24/6/1 respectively; the more even distribution of satellites in the six-plane patterns is evident from these figures.

Initial approaches to this problem in the USA have been described by Book *et al*[10] and by Jorgensen[13]. The obvious first approach was to retain a three-plane configuration but with the optimum uniform distribution of six instead of eight satellites in each plane, *i.e.* to change from delta pattern 24/3/2 to delta pattern 18/3/0. However, though this gave fairly uniform coverage, the performance provided in terms of the navigation criterion PDOP was poor.

Book *et al* then investigated other distributions of 18 satellites in three planes, and identified a non-uniform pattern which provided better performance in terms of the navigation criterion PDOP; this corresponded to the original delta pattern 24/3/2 with two satellites removed from each of the three planes and the remainder left in their original positions. As noted in Appendix A and Table 7 of Ref 4, in 12-hour orbits pattern 24/3/2 would follow eight separate Earth-tracks, while 18/3/0 would follow six

and 18/6/2 would follow nine; the six satellites removed from 24/3/2 would correspond to those following two adjacent tracks, leaving six tracks only. This non-uniform 18-satellite three-plane pattern is illustrated by the circle symbols in Fig 12a, with the crosses representing the satellites removed from pattern 24/3/2. It may be noted that the values of D_{Min} at 55° for these patterns are: 24/3/2 - 10.8° (λ = 0.242); 18/3/0 - 20.8° (λ = 0.404); while the non-uniform 18-satellite three-plane pattern has the same value of D_{Min} as 24/3/2 from which it is derived, *ie* 10.8° (λ = 0.210). The orders of merit given by PDOP and λ are therefore contradictory in this case; this may be partly explained by the fact that λ deals with worst-case conditions, whereas PDOP is statistical in nature and can overlook isolated adverse cases. When a pattern is uniformly 'good', it is likely to be recognised as such by both λ and PDOP; whereas, given a choice between one which is uniformly 'mediocre' and one which is sometimes 'good' and sometimes 'poor', the former will be favoured by λ and the latter by PDOP.

Another non-uniform 18-satellite constellation was subsequently proposed by Blake[13,14]. In Ref 4 it was remarked that other authors had apparently not recognised single-satellite-per-plane patterns as important members of the family of delta patterns; these were subsequently discussed by Ballard[12] under the title of 'rosette constellations', and Blake's proposal was for a 'modified rosette' in which six evenly-spaced satellites were removed from the delta (or rosette) pattern 24/24/2 (*ie* one from every fourth plane) and the phase spacing (but not the longitude spacing) of the remainder was then adjusted to be the same as that for pattern 18/18/2, *ie* phase difference between adjacent planes changed from 30° to 40°. Pattern 24/24/2 (with the six satellites removed indicated by crosses and those remaining indicated by circles) and Blake's 18-satellite modified rosette derived from it are illustrated in Fig 13a&b respectively. Jorgensen[15] has indicated that, in terms of percentage visibility and cumulative accuracy probability, the modified rosette gives slightly better results than the non-uniform three-plane pattern, but that pattern 18/6/2 appears superior to both. It may be noted that D_{Min} for pattern 24/24/2, and for the 18-satellite pattern left when six satellites are removed from it, is 12.0° (λ = 0.233 for 18 satellites); for Blake's modified rosette with adjusted spacing it is 18.4° (λ = 0.358); and for pattern 18/6/2 it is 33.3° (λ = 0.647). The λ values therefore agree with Jorgensen's order of merit in these cases.

It appeared to the present writer that Blake's proposal might be capable of further development; this led to the brief study[7] whose results are described in the following section.

5.2 Non-uniform patterns

Some larger delta patterns, involving a total number of satellites (T) which is not a prime number, may be regarded as being built up from several similar delta sub-patterns, evenly spaced; and some patterns which are not themselves delta patterns may nevertheless also be regarded as being built up from several similar delta sub-patterns, though with these not all evenly spaced. Thus pattern 24/24/2 may be regarded as built up of four examples of pattern 6/6/2, spaced by 15° in longitude and by 30° in phase. Blake's modified rosette consists of three examples of pattern 6/6/2, spaced by

15° in longitude (with one 30° gap) and by 40° in phase; clearly in such a case the phase spacing of the sub-patterns could take any suitable value. In the initial account[7] of this study the name 'omega patterns' was adopted for such non-uniform patterns built up from delta sub-patterns; and, considering specifically those which have evenly-spaced omissions from an otherwise even spacing of planes in a rosette pattern, an omega pattern identification code T/P/F/W was adopted, based on the delta pattern identification code T/P/F, which is retained for the delta sub-pattern in the form $T_S/P_S/F_S$. In the omega pattern code T/P/F/W, T is the actual number of satellites in the pattern (after any deletions); P is the total number of planes, both occupied and empty, corresponding to the even spacing of the occupied planes; F is the same as the value of F_S for the sub-pattern; and W, expressed in units of $360^\circ/P$, is the phase spacing between the sub-patterns, measured in the same sense as F, and can take any real value from 0 to P (with W = P equivalent to W = 0). Note that $P_S = T_S$ is equal to the value of (P - T) for the omega pattern, which must be a factor of both T and P.

Using this identification code, removing one of the four 6/6/2 sub-patterns from the delta pattern 24/24/2 leaves the omega pattern 18/24/2/2.0, while changing the phase spacing between the sub-patterns from 30° to 40° in accordance with Blake's proposal produces the omega pattern 18/24/2/2.667.

Clearly the characteristics of an omega pattern are partly determined by those of the delta sub-pattern from which it is built up and, in particular, the value of D_{Min} for an omega pattern cannot exceed that for the sub-pattern at the same inclination. Hence, if the sub-pattern has $D_{Min} = 0^\circ$, any omega pattern based on it will also have $D_{Min} = 0^\circ$; and it appears unwise to choose a sub-pattern having a value of D_{Min} substantially less than that of the delta pattern giving the largest value of D_{Min} for the value of T to be used for the omega pattern (*eg* 38.1° for 18 satellites), since the sub-pattern would then probably be the limiting factor on the value of D_{Min} for the omega pattern.

Considering all possible 24-satellite rosette patterns composed of 6-satellite rosette sub-patterns, we find that there are six possible sub-patterns which between them produce 24 rosette patterns, each of which leaves an omega pattern when one sub-pattern is deleted; these are identified as follows:

Sub-pattern $T_S/P_S/F_S$	Rosette pattern T/P/F	Omega pattern T/P/F/W	Sub-pattern $T_S/P_S/F_S$	Rosette pattern T/P/F	Omega pattern T/P/F/W
6/6/0	24/24/0	18/24/0/0.0	6/6/3	24/24/3	18/24/3/3.0
	24/24/6	18/24/0/6.0		24/24/9	18/24/3/9.0
	24/24/12	18/24/0/12.0		24/24/15	18/24/3/15.0
	24/24/18	18/24/0/18.0		24/24/21	18/24/3/21.0
6/6/1	24/24/1	18/24/1/1.0	6/6/4	24/24/4	18/24/4/4.0
	24/24/7	18/24/1/7.0		24/24/10	18/24/4/10.0
	24/24/13	18/24/1/13.0		24/24/16	18/24/4/16.0
	24/24/19	18/24/1/19.0		24/24/22	18/24/4/22.0
6/6/2	24/24/2	18/24/2/2.0	6/6/5	24/24/5	18/24/5/5.0
	24/24/8	18/24/2/8.0		24/24/11	18/24/5/11.0
	24/24/14	18/24/2/14.0		24/24/17	18/24/5/17.0
	24/24/20	18/24/2/20.0		24/24/23	18/24/5/23.0

Thus, for the omega patterns, when we come to consider values of D_{Min} over the full range of values of W from 0 to 23.999, we know that for each value of F there are four particular values of W at which the value of D_{Min} will be the same as for the corresponding rosette pattern and that, for all values of W, D_{Min} will not exceed the value for the sub-pattern.

From section 3.5 of Ref 4 we know that a delta pattern will have $D_{Min} = 0^\circ$ if both P and (T/P - F) are even numbers. Here this applies to the delta sub-patterns 6/6/1, 6/6/3 and 6/6/5, and to all the rosette and omega patterns based upon them; these may therefore be excluded from further discussion.

For sub-pattern 6/6/2 we have already (in the previous section) noted values of D_{Min} (at 55° inclination) at W = 2.0 and 2.667; the values at W = 8.0, 14.0 and 20.0 correspond to those for the other three rosette patterns, and we may calculate further values of D_{Min} at intermediate values of W to obtain the complete picture of the variation of D_{Min} with W. We find that D_{Min} falls from 6.1° at W = 0 to 4.4° at 1.0, then rises to 12.0° at 2.0, 15.2° at 2.333, 18.4° at 2.667, and 21.3° (the limiting value for sub-pattern 6/6/2) at 3.0. It then falls to 18.2° at W = 3.333, 6.1° at 4.0, 12.2° at 5.0, 0.3° at 6.0, and rises again to the limiting value of 21.3° at 7.0, 7.25 and 7.5, before falling to 19.7° at 8.0, 11.2° at 9.0 and 0.3° at 10.0. Similar fluctuations of D_{Min} continue across the rest of the range of values of W. Thus we see that we can improve on the value of D_{Min} of 18.4° at the value of W proposed by Blake, reaching the limiting value of 21.3° for values of W in the neighbourhood of 3.0 and 7.25. Values of PDOP would not necessarily vary in similar manner, but their behaviour would appear worth investigating. Satellite positions in these patterns are listed in Table 18, and pattern 18/24/2/7.25 is shown in Fig 13c.

Sub-patterns 6/6/0 and 6/6/4, on the other hand, have values of D_{Min} of 33.3° and 70.0° respectively at 55° inclination; there is therefore some prospect that omega patterns based on either of these might prove superior to those based on sub-pattern 6/6/2. A limited investigation was made of omega patterns based on sub-pattern 6/6/4. From the rosette patterns, we find that $D_{Min} = 6.1^\circ$ at W = 4.0, 2.4° at 10.0, 6.1° at 16.0 and 21.2° at 22.0; near the latter value of W, it falls to 18.3° at 22.2, but rises to 24.2° at 21.8 and to a peak of 28.1° at W = 21.541 before falling to 24.0° at 21.4, 12.2° at 21.0 and 2.4° at 20.5, then rising to a smaller peak at 26.8° at W = 19.667. Thus a D_{Min} of at least 28.1° can be obtained by changing to a different sub-pattern. Satellite positions in these patterns are listed in Table 19, and pattern 18/24/4/21.541 is shown in Fig 13d. This is particularly interesting in that it shows that, in optimising for D_{Min}, we have arrived at a 24-plane pattern (shown by circles) which matches very closely (though not exactly) the delta pattern 18/18/6 (shown by ×s) which was one of the short-list of seven whose characteristics were quoted in the previous section.

We have thus far followed Blake in assuming that we should look for an 18-satellite omega pattern expandable to a 24-satellite rosette pattern. However, there are some advantages, in the circumstances described in the preceding section, in considering an 18-satellite omega pattern based on a 21-satellite rosette pattern, as in optimising the

system at the 21-satellite level rather than at the 24-satellite level. A 21-satellite delta pattern may be considered to be composed of seven 3-satellite sub-patterns; to meet the requirement under discussion, any six of these sub-patterns may be active and any one the inactive spare set. Different sub-patterns could be designated as the spare set in turn at different times, so equalising satellite life expectancy over the whole system, and when any one satellite failed the set of which it formed part could be designated as the spare set until a replacement had been launched, thus completely 'hiding' a single satellite failure (though such changes would require some re-adjustment of phasing among the active satellites if the value of W did not correspond directly to a rosette pattern). Hence, though a 21-plane 18-satellite pattern provides a less satisfactory basis than a 24-plane 18-satellite pattern for possible later expansion to a 24-satellite system, since this would have to be non-uniform, the 21-plane constellation seems likely to provide a more failure-resistant system at the more critical initial stage when only 18 satellites would be active, with three inactive spares.

Of the 21-plane delta (rosette) patterns which might form a basis for such a system, the two most promising are probably 21/21/9 and 21/21/19. At 55° inclination 21/21/19, and hence also the omega pattern 18/21/1/19.0, has D_{Min} = 24.2°; this is increased as W is reduced, with a maximum of D_{Min} = 28.1° for pattern 18/21/1/18.772. At the same inclination 21/21/9, and hence also the omega pattern 18/21/0/9.0 (see Table 20 and Fig 13e), has D_{Min} = 30.4°. This is at least a local maximum, D_{Min} falling as W is either increased or decreased from the value W = 9.0; the satellites would not (since W is unchanged from the rosette pattern) need phase adjustments when sub-patterns changed between active and inactive status; and this local maximum may be the largest value of D_{Min} obtainable with a 21-plane 18-satellite pattern (though not all values of W over the full range from 0 to 20.999 have been checked to confirm this). Indeed, the example of pattern 18/24/4/21.541 raises the possibility that a 21-plane pattern might be found which would closely match the delta pattern 18/9/6, though this has not been pursued further.

Thus the largest values of D_{Min} for 18-satellite constellations at 55° inclination which we have found during this brief study using the non-uniform omega patterns are 30.4° for the 21-plane pattern 18/21/0/9.0 and 28.1° for the 24-plane pattern 18/24/4/21.541. These values compare with values for the uniform delta patterns of 33.3° for the six-plane pattern 18/6/2, 28.2° for the 18-plane pattern 18/18/16, and 20.8° for the three-plane pattern 18/3/0. Of these patterns, positioning of three inactive spares and bringing them into service after a failure appears to be most readily accomplished in patterns 18/21/0/9.0, 18/6/2 and 18/3/0, while expansion to 24 satellites would be most readily performed with patterns 18/24/4/21.541, 18/6/2 and 18/3/0. Overall, delta pattern 18/6/2 may well be considered to have most advantages (though some other relevant factors, such as launching arrangements, have not been considered here); Brady and Jorgensen[16] indicated that, in 1981, this pattern was (subject to some further consideration of possible advantages of a three-plane pattern as regards Shuttle launching) the current baseline orbital configuration for the operational Phase III GPS.

6 CONCLUSIONS

This Report has described several separate, though related, studies performed during the period 1977-1982. The principal conclusions emerging from these studies are as follows:

(1) An examination of the coverage characteristics of regular tesselations of an infinite plane and of regular polyhedra has led to:

(a) the identification of trends, with respect to numbers of satellites and degrees of coverage, which appear applicable also to practical constellations of satellites in Earth orbit;

(b) the use of alternative versions ($1/c_n$ and c_n), normalised by reference to the characteristics of an ideal triangular tesselation, of the criteria ($R_{MAX,n}$ and D_{MIN}) which have been used in previous coverage studies; and hence

(c) the formulation of methods of predicting approximate values of these criteria which may be expected to be achievable with larger numbers of satellites and higher degrees of coverage than have yet been examined in detail for practical satellite constellations.

(2) An attempt to produce a combined criterion incorporating both $R_{MAX,n}$ and D_{MIN} has demonstrated the much stronger influence of D_{MIN}, and suggests that it would be appropriate to use D_{MIN}, which is much the simpler to calculate, as the sole criterion in drawing up a short-list of orbital patterns for detailed study against any particular coverage requirement.

(3) It has been confirmed that the delta patterns giving the largest values of D_{MIN} are those which produce single non-self-crossing Earth-tracks at certain altitudes; these patterns can be identified by methods which were developed in a previous report[4].

(4) An examination of non-uniform patterns, using D_{MIN} as criterion, has suggested:

(a) that it is possible to improve on results obtained elsewhere by choosing the most suitable sub-pattern and then optimising the phasing between adjacent planes, and

(b) that in a non-uniform system including both active satellites and spares in orbit, it may be desirable to optimise for the total number of satellites in orbit.

(5) Results obtained in section 5 have been discussed with reference to the requirements of the GPS navigation satellite system. Subject to satisfactory launching arrangements being determined, it appears that the delta pattern 18/6/2, to which attention was originally drawn in Appendix A of Ref 4, may well have most overall advantages among potential 18-satellite constellations, and it is understood to have been selected by the programme authorities as the GPS baseline.

Table 1

EXAMPLE LISTS OF CIRCUMCIRCLES FOR TRIANGULAR TESSELATION

Fig 3a			Fig 3b		
Circle	Radius/L	x, y	Circle	Radius/L	x, y
A	0.5774	3, 0	D	1.3229	4, 4
B	1.0000	6, 1	E	1.3472	3, 5
E	1.3472	3, 5	F	1.4000	3, 6
G	1.5276	6, 6	G	1.5276	6, 6
K	1.8028	4, 10	J	1.7500	3, 9
S	2.0817	6, 12	L	1.8359	4, 10
V	2.1939	3, 16	P	1.9079	4, 12
α	2.3065	4, 17	R	2.0207	3, 14
π	2.6458	12, 19	U	2.1824	3, 15
			W	2.2194	4, 16
			Z	2.2944	3, 18
			δ	2.3472	3, 19
			π	2.6458	12, 19

Table 2

DERIVATION OF VALUES OF $R_{MAX,n}$ FOR TRIANGULAR TESSELATIONS

Circle	Radius/L	x, y	Relevant values of n
A	0.5774	3, 0	1
B	1.0000	6, 1	2 3 4 5
C	1.1547	3, 3	4
D	1.3229	4, 4	5 6
E	1.3472	3, 5	6
F	1.4000	3, 6	7
G	1.5276	6, 6	7 8 9 10
H	1.7321	6, 7	8 9 10 11
J	1.7500	3, 9	10
K	1.8028	4, 10	11 12
L	1.8359	4, 10	11 12
M	1.8571	3, 11	12
N	1.8764	3, 12	13
P	1.9079	4, 12	13 14
Q	2.0000	6, 13	14 15 16 17
R	2.0207	3, 14	15
S	2.0817	6, 12	13 14 15 16
T	2.1794	4, 14	15 16
U	2.1824	3, 15	16
V	2.1939	3, 16	17
W	2.2194	4, 16	17 18
X	2.2452	4, 16	17 18
Y	2.2913	4, 18	19 20
Z	2.2944	3, 18	19
α	2.3065	4, 17	18 19
β	2.3094	3, 18	19
γ	2.3333	3, 18	19
δ	2.3472	3, 19	20
ε	2.3750	3, 20	21
ζ	2.3848	4, 19	20 21
η	2.4249	3, 20	21
θ	2.4459	3, 21	22
λ	2.5018	3, 22	23
μ	2.5166	6, 21	22 23 24 25
ξ	2.6000	3, 23	24
π	2.6458	12, 19	20 21 22 23 24 25 26 27 28 29
ρ	2.6674	3, 24	25
σ	2.6943	3, 25	26
φ	2.7143	3, 25	26
ψ	2.7538	4, 25	26 27
ω	2.7839	4, 26	27 28

Table 3

DERIVATION OF VALUES OF $R_{MAX,n}$ FOR SQUARE TESSELATIONS

Circle	Radius/L	x, y	Relevant values of n
A	0.7071	4, 0	1 2
B	1.0000	4, 1	2 3
C	1.1180	4, 2	3 4
D	1.1785	3, 3	4
E	1.2500	3, 4	5
F	1.4142	4, 5	6 7
G	1.5811	8, 4	5 6 7 8 9 10
H	1.6667	3, 7	8
J	1.7678	3, 8	9
K	1.8028	4, 8	9 10
L	1.8211	3, 9	10
M	1.8385	3, 10	11
N	1.9003	4, 10	11 12
P	2.0000	4, 9	10 11
Q	2.0156	4, 10	11 12
R	2.0616	4, 12	13 14
S	2.0825	3, 12	13
T	2.1024	4, 11	12 13
U	2.1213	4, 12	13 14
V	2.1250	3, 12	13
W	2.1368	3, 13	14
X	2.1667	3, 14	15
Y	2.1731	4, 13	14 15
Z	2.2361	8, 13	14 15 16 17 18 19
α	2.2535	3, 15	16
β	2.3049	4, 14	15 16
γ	2.3570	3, 15	16
δ	2.5000	6, 16	17 18 19 20

Table 4

DERIVATION OF VALUES OF $R_{MAX,n}$ FOR HEXAGONAL TESSELATIONS

Circle	Radius/L	x, y	Relevant values of n
B	1.0000	3, 1	2
B'	1.0000	6, 0	1 2 3 4
D	1.3229	3, 2	3
D'	1.3229	4, 2	3 4
F	1.4000	3, 3	4
G	1.5276	4, 4	5 6
H	1.7321	6, 4	5 6 7 8
J	1.7500	3, 6	7
K	1.8028	4, 6	7 8
L	1.8359	3, 7	8
M	1.8571	3, 8	9
P	1.9079	4, 8	9 10
Q	2.0000	6, 6	7 8 9 10
Q'	2.0000	3, 10	11
S	2.0817	4, 8	9 10
T	2.1794	4, 10	11 12
W	2.2194	3, 10	11
X	2.2452	4, 9	10 11
Y	2.2913	4, 11	12 13
Z	2.2944	3, 11	12
α	2.3065	4, 10	11 12
γ	2.3333	3, 11	12
γ'	2.3333	3, 12	13
δ	2.3472	3, 12	13
ε	2.3750	3, 13	14
ζ	2.3848	4, 12	13 14
η	2.4249	3, 13	14
ξ	2.6000	3, 15	16
π	2.6458	6, 13	14 15 16 17
π'	2.6458	12, 12	13 14 15 16 17 18 19 20 21 22
φ	2.7143	3, 17	18
ψ	2.7538	3, 16	17
ω	2.7839	4, 16	17 18

Table 5

DERIVATION OF $1/c_n$: REGULAR TESSELATIONS

n	$R_{MAX,n}/L$			c_n			$1/c_n$		
	T	S	H	T	S	H	T	S	H
1	0.5774	0.7071	1.0000	1.0997	1.2533	1.5551	0.9093	0.7979	0.6430
2	1.0000	1.0000	1.0000	1.3468	1.2533	1.0996	0.7425	0.7979	0.9094
3	1.0000	1.1180	1.3229	1.0996	1.1441	1.1878	0.9094	0.8741	0.8419
4	1.1547	1.1785	1.4000	1.0996	1.0444	1.0886	0.9094	0.9597	0.9186
5	1.3229	1.5811	1.7321	1.1268	1.2533	1.2046	0.8875	0.7979	0.8301
6	1.3472	1.5811	1.7321	1.0475	1.1441	1.0997	0.9546	0.8741	0.9094
7	1.5276	1.5811	2.0000	1.0997	1.0592	1.1756	0.9093	0.9441	0.8507
8	1.7321	1.6667	2.0000	1.1664	1.0444	1.0996	0.8574	0.9574	0.9094
9	1.7321	1.8028	2.0817	1.0997	1.0651	1.0791	0.9094	0.9389	0.9267
10	1.7500	2.0000	2.2452	1.0540	1.1210	1.1041	0.9488	0.8921	0.9057
11	1.8359	2.0156	2.3065	1.0543	1.0772	1.0815	0.9485	0.9284	0.9247
12	1.8571	2.1024	2.3333	1.0211	1.0757	1.0475	0.9794	0.9296	0.9547
13	2.0817	2.1250	2.6458	1.0997	1.0446	1.1412	0.9094	0.9573	0.8763
14	2.0817	2.2361	2.6458	1.0597	1.0593	1.0997	0.9437	0.9441	0.9094
15	2.1794	2.3049	2.6458	1.0718	1.0548	1.0624	0.9330	0.9480	0.9413
16	2.1824	2.3570	2.6458	1.0392	1.0444	1.0286	0.9623	0.9575	0.9722
17	2.2453			1.0371			0.9642		
18	2.3065			1.0354			0.9658		
19	2.3333			1.0195			0.9808		
20	2.6458			1.1268			0.8875		
21	2.6458			1.0997			0.9094		
22	2.6458			1.0744			0.9308		
23	2.6458			1.0508			0.9517		
24	2.6458			1.0286			0.9722		
25	2.6674			1.0161			0.9842		
∞				1.0000	1.0000	1.0000	1.0000	1.0000	1.0000

T = triangular tesselation
S = square tesselation
H = hexagonal tesselation

Table 6

EXAMPLE LISTS OF CIRCUMCIRCLES FOR OTHER TESSELATIONS

Circle	Radius/l.	x, y									
		Tri-hex A		Tri-hex B							Rectangle
D	1.3229	4, 3	4, 3	3, 3	3, 3	3, 3	3, 3	4, 3	4, 2	4, 3	4, 2
E	1.3472		3, 4	3, 4	3, 3		3, 3	3, 4	3, 3		
F	1.4000		3, 5	3, 5	3, 4	3, 4	3, 4		3, 4	3, 4	
G	1.5276	6, 3	4, 5	4, 5	6, 4	6, 4	4, 5	6, 4	4, 5	4, 4	4, 2
J	1.7500	3, 6	3, 6		3, 7		3, 7	3, 7	3, 7	3, 5	3, 3
L	1.8359	3, 7	4, 7	4, 6		3, 7	4, 8	3, 8	3, 8	4, 6	3, 4
P	1.9079	4, 8	3, 9	4, 8	4, 8	4, 8		3, 9	3, 9	4, 8	3, 5
R	2.0207	3, 10	3, 10	3, 10	3, 10	3, 10	3, 10	3, 10	3, 10	3, 10	3, 6
U	2.1824		3, 11	3, 11		3, 11	3, 11	3, 11	3, 11		
W	2.2194	4, 11	3, 12	4, 12	4, 11	4, 12	3, 12	3, 12	4, 12	4, 11	3, 7
Z	2.2944	3, 13			3, 13	3, 14		3, 13	3, 14		
δ	2.3472	3, 14			3, 14	3, 15	3, 13		3, 15	3, 13	
π	2.6458	8, 14	12, 12	12, 13	8, 15	8, 15	12, 13	12, 13	8, 15	8, 14	8, 8

Table 7

DERIVATION OF $1/c_n$: OTHER TESSELATIONS

n	$R_{MAX,n}/L$			c_n			$1/c_n$		
	T-h A	T-h B	R	T-h A	T-h B	R	T-h A	T-h B	R
1	1.0000	1.0000	1.0000	1.6494	1.6494	1.3468	0.6063	0.6063	0.7425
2	1.0000	1.0000	1.1547	1.1663	1.1663	1.0996	0.8574	0.8574	0.9094
3	1.1547	1.3229	1.5276	1.0996	1.2598	1.1878	0.9094	0.7938	0.8419
4	1.5276	1.3472	1.7500	1.2598	1.1111	1.1784	0.7937	0.9000	0.8486
5	1.5276	1.5276	1.8764	1.1268	1.1268	1.1302	0.8874	0.8874	0.8848
6	1.7321	1.7500	2.0000	1.1664	1.1784	1.0996	0.8574	0.8486	0.9094
7	1.7500	1.8359	2.1794	1.0910	1.1446	1.1094	0.9166	0.8737	0.9014
8	1.8571	1.8571	2.3848	1.0830	1.0830	1.1355	0.9234	0.9234	0.8806
9	1.9079	2.0817	2.6458	1.0490	1.1446	1.1878	0.9533	0.8737	0.8419
10	2.0817	2.0817	2.6943	1.0858	1.0858	1.1475	0.9210	0.9210	0.8715
11	2.1794	2.1794	2.7839	1.0839	1.0839	1.1305	0.9226	0.9226	0.8846
12	2.2913	2.2194	2.7839	1.0910	1.0508	1.0823	0.9166	0.9463	0.9239
13	2.6458	2.6458		1.2104	1.2104		0.8262	0.8262	
14	2.6458	2.6458		1.1664	1.1664		0.8574	0.8574	
15	2.6458	2.6458		1.1268	1.1268		0.8875	0.8875	
16	2.6458	2.64-		1.0910	1.0910		0.9166	0.9166	

Table 8

DERIVATION OF VALUES OF $R_{MAX,n}$ FOR REGULAR POLYHEDRA

Polyhedron	Radius (deg)	x, y	Relevant values of n
Tetrahedron	70.5288	3, 0	1
	109.4712	3, 1	2
Octahedron	54.7356	3, 0	1
	90.0000	4, 1	2, 3
	125.2644	3, 3	4
Cube	54.7356	4, 0	1 (2)
	70.5288	3, 1	2
	90.0000	4, 2	3, 4
	109.4712	3, 4	(5)
	125.2644	4, 4	5, 6
Icosahedron	37.3774	3, 0	1
	63.4350	5, 1	2, 3 (4)
	79.1877	3, 3	4
	90.0000	4, 4	5, 6
	100.8123	3, 6	(7)
	116.5650	5, 6	7, 8, 9
	142.6226	3, 9	10
Dodecahedron	37.3774	5, 0	1 (2, 3)
	41.8103	3, 1	2
	54.7356	4, 2	3 (4)
	56.7949	3, 3	4
	60.7941	3, 4	(5)
	70.5288	6, 4	5 (6, 7, 8)
	79.1877	5, 5	6, 7, 8
	90.0000	4, 8	9, 10
	100.8123	5, 10	(11, 12, 13)
	109.4712	6, 10	11, 12, 13 (14)
	119.2059	3, 13	14
	123.2051	3, 14	(15)
	125.2644	4, 14	15 (16)
	138.1897	3, 16	(17)
	142.6226	5, 15	16, 17, 18

Table 9

DERIVATION OF $1/c_n$: REGULAR POLYHEDRA

Polyhedron	n	$R_{MAX,n}$ (deg)	c_n	$1/c_n$
Tetrahedron	1	70.5288	1.2310	0.8124
	2	109.4712	1.3510	0.7402
Octahedron	1	54.7356	1.1700	0.8547
	2	90.0000	1.3603	0.7351
	3	90.0000	1.1107	0.9003
	4	125.2644	1.3388	0.7469
Cube	1	54.7356	1.3510	0.7402
	2	70.5288	1.2310	0.8124
	3	90.0000	1.2825	0.7797
	4	90.0000	1.1107	0.9003
	5	125.2644	1.3827	0.7232
	6	125.2644	1.2622	0.7922
Icosahedron	1	37.3774	1.1299	0.8850
	2	63.4350	1.3560	0.7375
	3	63.4350	1.1071	0.9032
	4	79.1877	1.1969	0.8355
	5	90.0000	1.2167	0.8219
	6	90.0000	1.1107	0.9003
	7	116.5650	1.3319	0.7508
	8	116.5650	1.2458	0.8027
	9	116.5650	1.1746	0.8514
	10	142.6226	1.3634	0.7335
Dodecahedron	1	37.3774	1.4587	0.6855
	2	41.8103	1.1538	0.8667
	3	54.7356	1.2333	0.8108
	4	56.7949	1.1083	0.9023
	5	70.5288	1.2310	0.8124
	6	79.1877	1.2617	0.7926
	7	79.1877	1.1681	0.8561
	8	79.1877	1.0926	0.9152
	9	90.0000	1.1708	0.8541
	10	90.0000	1.1107	0.9003
	11	109.4712	1.2881	0.7763
	12	109.4712	1.2333	0.8108
	13	109.4712	1.1849	0.8439
	14	119.2039	1.2434	0.8043
	15	125.2644	1.2622	0.7922
	16	142.6226	1.3415	0.7456
	17	142.6226	1.3500	0.7408
	18	142.6226	1.3119	0.7622

Table 10

SMALLEST VALUES OF $R_{MAX,n}$ FOR DELTA PATTERNS

n	T	Pattern	$R_{MAX,n}$ (deg)	δ_{opt} (deg)	D_{Min} (deg)	ρ_n	$1/\rho_n$	λ	ε_n
1	5	5/5/1	69.2	43.7	60.9	1.350	0.741	0.624	0.462
	6	6/6/4	66.4	53.1	73.7	1.419	0.705	0.827	0.583
	7	7/7/5	60.3	55.7	57.0	1.392	0.718	0.691	0.496
	8	8/8/6	56.5	61.9	56.3	1.395	0.717	0.730	0.523
	9	9/9/7	54.8	70.5	43.1	1.435	0.697	0.592	0.413
	10	10/5/2	52.2	57.1	46.6	1.441	0.694	0.675	0.469
	11	11/11/4	47.6	53.8	49.0	1.378	0.726	0.745	0.540
	12	12/3/1	47.9	50.7	26.0	1.448	0.691	0.413	0.285
	13	13/13/5	43.8	58.4	45.9	1.378	0.726	0.758	0.550
	14	14/7/4	42.0	54.0	42.5	1.371	0.729	0.729	0.531
	15	15/3/1	42.1	53.5	20.2	1.423	0.703	0.358	0.252
2	7	7/7/2	76.0	61.8	37.1	1.241	0.806	0.450	0.362
	8	8/8/2	71.0	57.1	9.6	1.239	0.807	0.124	0.100
	9	9/3/2	66.2	62.1	24.2	1.225	0.816	0.333	0.271
	10	10/10/2	64.1	61.6	21.2	1.251	0.799	0.307	0.246
	11	11/11/9	62.0	52.7	44.1	1.269	0.788	0.670	0.528
	12	12/3/1	56.6	57.0	18.2	1.210	0.827	0.289	0.239
	13	13/13/3	54.7	52.8	38.0	1.217	0.822	0.628	0.516
	14	14/14/10	52.4	53.8	16.7	1.210	0.827	0.286	0.237
	15	15/3/1	51.3	55.3	21.5	1.226	0.816	0.369	0.301
3	10	10/10/8	80.3	60.0	51.5	1.279	0.782	0.746	0.583
	11	11/11/3	74.6	59.8	3.9	1.247	0.802	0.059	0.048
	12	12/4/2	70.9	60.0	5.4	1.237	0.808	0.086	0.069
	13	13/13/4	68.0	50.0	27.1	1.235	0.810	0.448	0.362
	14	14/14/4	66.1	47.6	4.6	1.246	0.803	0.079	0.063
	15	15/15/6	63.2	57.0	41.9	1.233	0.811	0.744	0.603
4	13	13/13/2	77.1	45.7	29.3	1.213	0.824	0.484	0.399
	14	14/14/4	75.8	69.6	4.3	1.238	0.808	0.074	0.060
	15	15/15/2	70.9	55.7	21.8	1.198	0.835	0.387	0.323
	18	18/3/0	65.1	57.5	17.6	1.205	0.830	0.342	0.284
	21	21/3/2	58.8	54.4	15.5	1.176	0.851	0.325	0.277
5	18	18/6/2	73.6	64.6	20.5	1.219	0.821	0.398	0.327
6	24	24/4/3	68.3	56.7	14.1	1.192	0.839	0.316	0.265
7	24	24/8/4	75.8	59.9	24.2	1.225	0.816	0.543	0.443

Table II

D_{MIN} FOR DELTA PATTERNS GIVING NON-SELF-CROSSING EARTH-TRACKS

T	L:M = 2:1				L:M = 3:2				L:M = 4:3				L:M = 5:4			
	Pattern	D_{MIN} (deg)	$\delta_{opt,D}$ (deg)	λ	Pattern	D_{MIN} (deg)	$\delta_{opt,D}$ (deg)	λ	Pattern	D_{MIN} (deg)	$\delta_{opt,D}$ (deg)	λ	Pattern	D_{MIN} (deg)	$\delta_{opt,D}$ (deg)	λ
5	5/5/3	82.2	51.8	0.842	5/5/1	72.0	0	0.738	5/5/2	72.0	0	0.738	5/5/0	72.0	0	0.738
6	6/6/4	73.7	53.1	0.828	6/3/0	60.0	0-54.7	0.673	6/2/0	60.0	0	0.673	6/3/2	60.0	0	0.673
7	7/7/5	68.3	58.6	0.828	7/7/2	58.9	48.0	0.714	7/7/1	51.4	0	0.623	7/7/4	51.4	0	0.623
8	8/8/6	61.9	59.1	0.802	8/4/1	56.4	48.1	0.731	8/8/4	45.0	0-57.2	0.583	8/2/1	45.0	0	0.583
9	9/9/7	57.9	62.7	0.795	9/9/3	54.9	50.9	0.754	9/3/2	45.8	46.5	0.629	9/9/1	40.0	0	0.550
10	10/10/8	53.1	63.4	0.770	10/5/2	53.1	53.1	0.770	10/10/2	44.3	43.4	0.642	10/5/0	36.0	0-58.3	0.522
11	11/11/9	50.1	66.2	0.761	11/11/4	50.1	53.1	0.761	11/11/6	43.0	43.0	0.653	11/11/7	37.4	45.8	0.568
12	12/12/10	46.5	66.8	0.738	12/6/3	48.2	54.7	0.764	12/4/0	42.0	44.2	0.667	12/3/1	36.6	41.2	0.581
13	13/13/11	44.1	68.9	0.728	13/13/5	47.3	57.6	0.781	13/13/3	41.7	46.3	0.689	13/13/2	35.6	39.4	0.588
14	14/14/12	41.3	69.4	0.707	14/7/4	44.5	57.3	0.762	14/14/8	41.3	48.2	0.707	14/7/1	34.7	39.0	0.595
15	15/15/13	39.6	71.9	0.703	15/15/6	42.6	58.1	0.756	15/5/1	39.3	47.7	0.698	15/15/10	34.1	39.5	0.605
16	16/16/14	37.1	71.5	0.680	16/8/5	41.4	59.9	0.759	16/16/4	38.0	48.1	0.696	16/4/3	33.7	40.7	0.618
17	17/17/15	35.5	72.9	0.671	17/17/7	39.8	60.7	0.752	17/17/10	37.2	49.2	0.702	17/17/3	33.7	41.4	0.637
18	18/18/16	33.7	73.2	0.655	18/9/6	38.1	61.0	0.741	18/6/2	36.7	50.9	0.714	18/9/2	33.7	44.0	0.655
19	19/19/17	32.4	74.4	0.647	19/19/8	36.9	62.1	0.738	19/19/5	35.8	51.7	0.715	19/19/13	32.3	43.4	0.645
20	20/20/18	30.8	74.6	0.631	20/10/7	36.0	63.5	0.737	20/20/12	34.4	51.7	0.705	20/5/0	31.3	43.4	0.641
21	21/21/19	29.7	75.6	0.624	21/21/9	34.4	63.5	0.723	21/7/3	33.4	52.1	0.702	21/21/4	30.6	43.9	0.642
22	22/22/20	28.4	75.8	0.610	22/11/8	33.3	64.1	0.716	22/22/6	32.7	53.1	0.704	22/11/3	30.2	44.7	0.649
23	23/23/21	27.4	76.	0.602	23/23/10	32.6	65.3	0.715	23/23/14	32.4	54.9	0.711	23/23/16	30.0	45.9	0.659
24	24/24/22	26.3	76.	0.590	24/12/9	31.4	65.5	0.705	24/8/4	31.4	54.7	0.705	24/6/1	29.9	47.3	0.671
25	25/25/23	25.5	77.6	0.584	25/25/11	30.4	65.8	0.696	25/25/7	30.4	54.8	0.696	25/25/5	28.9	47.0	0.662

Table 12

LARGEST VALUES OF D_{MIN} FOR DELTA PATTERNS

T	Pattern	D_{MIN} (deg)	λ	$\theta_{opt,D}$ (deg)	n	$R_{Max,n}$ (deg)	σ_n	$1/\sigma_n$	ϵ_n
5	5/5/3	82.2	0.842	51.8	1	75.5	1.474	0.679	0.571
6	6/6/4	73.7	0.828	53.1	1	66.4	1.420	0.704	0.583
7	7/7/5	68.3	0.828	58.6	1	60.7	1.401	0.714	0.591
					2	81.5	1.331	0.752	0.622
8	8/8/6	61.9	0.802	59.1	1	56.9	1.405	0.712	0.571
					2	74.0	1.292	0.774	0.621
9	9/9/7	57.9	0.795	62.7	1	55.1	1.441	0.694	0.552
					2	69.7	1.290	0.775	0.617
					3	86.1	1.302	0.768	0.611
10	10/5/2	53.1	0.770	53.1	1	53.1	1.467	0.682	0.525
					2	65.2	1.273	0.786	0.605
11	11/11/4	50.1	0.761	53.1	1	47.7	1.380	0.725	0.551
					2	72.1	1.476	0.678	0.516
					3	78.0	1.304	0.767	0.584
					4	86.5	1.252	0.799	0.608
12	12/6/3	48.2	0.764	54.7	1	54.9	1.658	0.603	0.461
					2	61.5	1.314	0.761	0.582
					3	72.6	1.267	0.789	0.603
13	13/13/5	47.3	0.781	57.6	1	44.1	1.389	0.720	0.562
					2	60.4	1.344	0.744	0.581
					3	75.4	1.370	0.730	0.570
					4	80.6	1.268	0.789	0.616
14	14/7/4	44.5	0.762	57.3	1	42.4	1.385	0.722	0.550
					2	60.0	1.385	0.722	0.550
					3	67.5	1.273	0.786	0.599
					4	77.1	1.259	0.794	0.605
15	15/15/6	42.6	0.756	58.1	1	46.6	1.575	0.635	0.480
					2	55.0	1.313	0.761	0.576
					3	63.4	1.237	0.808	0.611
					4	78.5	1.327	0.753	0.570
16	16/8/5	41.4	0.759	59.9	1	40.8	1.423	0.703	0.534
					2	53.5	1.320	0.758	0.575
					3	65.1	1.312	0.762	0.579
					4	70.8	1.235	0.810	0.615
					5	80.4	1.254	0.797	0.605

(continued on following page)

Table 12 (concluded)

T	Pattern	D_{MIN} (deg)	λ	$\theta_{opt,D}$ (deg)	n	$R_{Max,n}$ (deg)	σ_n	$1/\sigma_n$	ε_n
17	17/17/7	39.8	0.752	60.7					
18	18/9/6	38.1	0.741	61.0	1	40.8	1.512	0.662	0.490
					2	50.2	1.313	0.762	0.564
					3	60.7	1.298	0.771	0.571
					4	69.0	1.277	0.783	0.580
					5	75.6	1.252	0.799	0.592
					6	82.7	1.250	0.800	0.592
19	19/19/8	36.9	0.738	62.1	1	38.8	1.475	0.678	0.500
					2	49.8	1.341	0.746	0.550
					3	61.5	1.351	0.740	0.546
					4	65.5	1.245	0.803	0.592
					5	72.9	1.240	0.806	0.595
					6	82.5	1.282	0.780	0.576
					7	86.2	1.239	0.807	0.595
20	20/10/7	36.0	0.737	63.5	1	38.4	1.498	0.667	0.492
					2	48.7	1.343	0.745	0.549
					3	60.8	1.371	0.730	0.538
					4	63.9	1.247	0.802	0.591
					5	72.3	1.262	0.793	0.584
					6	77.4	1.233	0.811	0.598
					7	84.6	1.247	0.802	0.591
21	21/21/9	34.4	0.723	63.5	1	37.4	1.496	0.669	0.483
					2	46.6	1.317	0.759	0.549
					3	60.5	1.396	0.716	0.518
					4	61.6	1.233	0.811	0.586
					5	69.1	1.235	0.810	0.585
					6	75.5	1.233	0.811	0.586
					7	84.0	1.269	0.788	0.570
22	22/11/8	33.3	0.716	64.1					
23	23/23/10	32.6	0.715	65.3					
24	24/12/9	31.4	0.705	65.5	1	36.7	1.567	0.638	0.450
					2	43.6	1.317	0.759	0.535
					3	56.9	1.405	0.712	0.502
					4	60.1	1.284	0.779	0.549
					5	65.1	1.246	0.803	0.566
					6	70.6	1.232	0.812	0.572
					7	77.3	1.249	0.800	0.564
25	25/25/7	30.4	0.696	54.8					

Table 13

SECOND-LARGEST VALUES OF D_{MIN} FOR DELTA PATTERNS

T	Pattern	D_{MIN} (deg)	λ	$\delta_{opt,D}$ (deg)	n	$R_{Max,n}$ (deg)	ε_n	$1/\varepsilon_n$	ε_n
5	5/5/1	72.0	0.738	0	1	90	1.756	0.569	0.420
6	6/3/0	60.0	0.673	0-54.7	1	90			
7	7/7/2	58.9	0.714	48.0	1	66.9	1.543	0.648	0.462
					2	79.5	1.297	0.771	0.550
8	8/4/1	56.4	0.731	48.1	1	58.3	1.439	0.695	0.508
9	9/9/3	54.9	0.754	50.9	1	67.2	1.759	0.569	0.429
					2	72.3	1.339	0.747	0.563
					3	84.2	1.272	0.786	0.593
10	10/10/8	53.1	0.770	63.4	1	53.5	1.477	0.677	0.521
					2	66.2	1.292	0.774	0.596
					3	82.1	1.308	0.764	0.588
11	11/11/9	50.1	0.761	66.2	1	52.7	1.525	0.656	0.499
					2	63.8	1.306	0.766	0.583
					3	80.4	1.344	0.744	0.566
					4	87.9	1.272	0.786	0.598
12	12/12/10	46.5	0.738	66.8	1	51.2	1.547	0.646	0.477
					2	60.7	1.298	0.771	0.568
					3	75.8	1.322	0.756	0.558
					4	87.5	1.323	0.756	0.558
13	13/13/11	44.1	0.728	68.9	1	50.4	1.586	0.631	0.459
					2	58.8	1.309	0.764	0.556
					3	73.1	1.327	0.753	0.548
					4	85.8	1.349	0.741	0.540
14	14/14/12	41.3	0.707	69.4	1	49.4	1.613	0.620	0.439
					2	56.5	1.304	0.767	0.542
					3	69.5	1.309	0.764	0.540
					4	82.8	1.352	0.740	0.523
15	15/15/13	39.6	0.703	71.9	1	49.4	1.670	0.599	0.421
					2	55.6	1.328	0.753	0.529
					3	67.3	1.314	0.761	0.535
					4	80.9	1.367	0.732	0.514
16	16/16/4	38.0	0.696	48.1					
17	17/17/10	37.2	0.702	49.2					
18	18/6/2	36.7	0.714	50.9					
19	19/19/5	35.8	0.715	51.7					
20	20/20/12	34.4	0.705	51.7					
21	21/7/3	33.4	0.702	52.1					
22	22/22/6	32.7	0.704	53.1					
23	23/23/14	32.4	0.711	54.9	1	38.2	1.598	0.626	0.445
					2	48.1	1.424	0.702	0.499
					3	51.5	1.244	0.804	0.572
					4	57.4	1.202	0.832	0.592
					5	66.4	1.242	0.805	0.572
					6	71.9	1.228	0.814	0.579
					7	77.9	1.232	0.812	0.577
24	24/8/4	31.4	0.705	54.7	1	45.0	1.924	0.520	0.366
					2	45.0	1.362	0.734	0.518
					3	50.1	1.236	0.809	0.570
					4	58.2	1.244	0.804	0.567
					5	65.9	1.260	0.794	0.559
					6	69.5	1.214	0.824	0.581
					7	76.5	1.236	0.809	0.570
25	25/25/11	30.4	0.696	65.8					

Table 14

VALUES OF $1/c_n$ FOR USE IN PREDICTIONS

	For minimum $R_{MAX,n}$			For maximum D_{MIN}		
n \ P	0.20	0.26	0.34	0.24	0.32	0.43
1	0.8154	0.7600	0.6861	0.7785	0.7046	0.6031
2	0.8296	0.7784	0.7103	0.7955	0.7273	0.6336
3	0.8427	0.7955	0.7325	0.8112	0.7483	0.6617
4	0.8548	0.8112	0.7531	0.8257	0.7676	0.6878
5	0.8659	0.8257	0.7721	0.8391	0.7855	0.7118
6	0.8762	0.8391	0.7896	0.8515	0.8020	0.7339
7	0.8858	0.8515	0.8058	0.8629	0.8172	0.7544
8	0.8945	0.8629	0.8207	0.8734	0.8313	0.7733
9	0.9026	0.8734	0.8345	0.8832	0.8442	0.7907
10	0.9101	0.8832	0.8472	0.8922	0.8562	0.8068

Table 15

VALUES OF c_n^2 FOR USE IN PREDICTIONS

	For minimum $R_{MAX,n}$			For maximum D_{MIN}		
n \ P	0.20	0.26	0.34	0.24	0.32	0.43
1	1.504	1.731	2.124	1.650	2.014	2.749
2	1.453	1.650	1.982	1.580	1.890	2.491
3	1.408	1.580	1.864	1.520	1.786	2.284
4	1.369	1.520	1.763	1.467	1.697	2.114
5	1.334	1.467	1.677	1.420	1.621	1.974
6	1.303	1.420	1.604	1.379	1.555	1.857
7	1.274	1.379	1.540	1.343	1.497	1.757
8	1.250	1.343	1.485	1.311	1.447	1.672
9	1.227	1.311	1.436	1.282	1.403	1.599
10	1.207	1.282	1.393	1.256	1.364	1.536

Table 16

PREDICTED MAXIMUM VALUES OF D_{MIN}

T	Predicted value $\lambda = 0.99\ T^{-0.1}$ (deg)	Lower limit $\lambda = 0.96\ T^{-0.1}$ (deg)	Upper limit $\lambda = 1.01\ T^{-0.1}$ (deg)
26	30.6	29.7	31.2
27	29.9	29.0	30.5
28	29.3	28.4	29.9
29	28.7	27.8	29.2
30	28.1	27.2	28.6
31	27.5	26.7	28.1
32	27.0	26.2	27.6
33	26.5	25.7	27.1
34	26.0	25.3	26.6
35	25.6	24.8	26.1
36	25.2	24.4	25.7
37	24.8	24.0	25.3
38	24.4	23.6	24.9
39	24.0	23.3	24.5
40	23.6	22.9	24.1

Table 17

DELTA PATTERNS GIVING NON-SELF-CROSSING EARTH-TRACKS

T \ L:M	3:2	4:3	5:4	6:5
26	26/13/10	26/26/16	26/13/4	26/26/4
27	27/27/12	27/9/5	27/27/19	27/27/15
28	28/14/11	28/28/8	28/7/2	28/28/10
29	29/29/13	29/29/18	29/29/6	29/29/22
30	30/15/12	30/10/6	30/15/5	30/6/0
31	31/31/14	31/31/9	31/31/22	31/31/5
32	32/16/13	32/32/20	32/8/3	32/32/18
33	33/33/15	33/11/7	33/33/7	33/33/12
34	34/17/14	34/34/10	34/17/6	34/34/26
35	35/35/16	35/35/22	35/35/25	35/7/1
36	36/18/15	36/12/8	36/9/4	36/36/6
37	37/37/17	37/37/11	37/37/8	37/37/21
38	38/19/16	38/38/24	38/19/7	38/38/14
39	39/39/18	39/13/9	39/39/28	39/39/30
40	40/20/17	40/40/12	40/10/5	40/8/2

Table 18

SATELLITE LOCATIONS IN 24-PLANE PATTERNS (F_S = 2)

Longitude of ascending node (all patterns) (deg)	Satellite phase angle at zero pattern phase angle (deg)				
	24/24/2	18/24/2/2.0	18/24/2/2.667	18/24/2/3.0	18/24/2/7.25
0	0	0	0	0	0
15.0	30.0	30.0	40.0	45.0	108.75
30.0	60.0	60.0	80.0	90.0	217.5
45.0	90.0				
60.0	120.0	120.0	120.0	120.0	120.0
75.0	150.0	150.0	160.0	165.0	228.75
90.0	180.0	180.0	200.0	210.0	337.5
105.0	210.0				
120.0	240.0	240.0	240.0	240.0	240.0
135.0	270.0	270.0	280.0	285.0	348.75
150.0	300.0	300.0	320.0	330.0	97.5
165.0	330.0				
180.0	0	0	0	0	0
195.0	30.0	30.0	40.0	45.0	108.75
210.0	60.0	60.0	80.0	90.0	217.5
225.0	90.0				
240.0	120.0	120.0	120.0	120.0	120.0
255.0	150.0	150.0	160.0	165.0	228.75
270.0	180.0	180.0	200.0	210.0	337.5
285.0	210.0				
300.0	240.0	240.0	240.0	240.0	240.0
315.0	270.0	270.0	280.0	285.0	348.75
330.0	300.0	300.0	320.0	330.0	97.5
345.0	330.0				
D_{Min}	12.0°	12.0°	18.4°	21.3°	21.3°

Table 19

SATELLITE LOCATIONS IN 24-PLANE PATTERNS (F_S = 4)

Longitude of ascending node (all patterns) (deg)	Satellite phase angle at zero pattern phase angle (deg)			
	24/24/22	18/24/4/22.0	18/24/4/21.541	18/24/4/19.667
0	0	0	0	0
15.0	330.0	330.0	323.1	295.0
30.0	300.0	300.0	286.2	230.0
45.0	270.0			
60.0	240.0	240.0	240.0	240.0
75.0	210.0	210.0	203.1	175.0
90.0	180.0	180.0	166.2	110.0
105.0	150.0			
120.0	120.0	120.0	120.0	120.0
135.0	90.0	90.0	83.1	55.0
150.0	60.0	60.0	46.2	350.0
165.0	30.0			
180.0	0	0	0	0
195.0	330.0	330.0	323.1	295.0
210.0	300.0	300.0	286.2	230.0
225.0	270.0			
240.0	240.0	240.0	240.0	240.0
255.0	210.0	210.0	203.1	175.0
270.0	180.0	180.0	166.2	110.0
285.0	150.0			
300.0	120.0	120.0	120.0	120.0
315.0	90.0	90.0	83.1	55.0
330.0	60.0	60.0	46.2	350.0
345.0	30.0			
D_{Min}	21.2°	21.2°	28.1°	26.8°

Table 20

SATELLITE LOCATIONS IN 21-PLANE PATTERNS

Longitude of ascending node (all patterns) (deg)	Satellite phase angle at zero pattern phase angle (deg)				
	21/21/19	18/21/1/19.0	18/21/1/18.772	21/21/9	18/21/0/9.0
0	0	0	0	0	0
17.1	325.7	325.7	321.8	154.3	154.3
34.3	291.4	291.4	283.6	308.6	308.6
51.4	257.1	257.1	245.4	102.9	102.9
68.6	222.9	222.9	207.2	257.1	257.1
85.7	188.6	188.6	169.0	51.4	51.4
102.9	154.3			205.7	
120.0	120.0	120.0	120.0	0	0
137.1	85.7	85.7	81.8	154.3	154.3
154.3	51.4	51.4	43.6	308.6	308.6
171.4	17.1	17.1	5.4	102.9	102.9
188.6	342.9	342.9	327.2	257.1	257.1
205.7	308.6	308.6	289.0	51.4	51.4
222.9	274.3			205.7	
240.0	240.0	240.0	240.0	0	0
257.1	205.7	205.7	201.8	154.3	154.3
274.3	171.4	171.4	163.6	308.6	308.6
291.4	137.1	137.1	125.4	102.9	102.9
308.6	102.9	102.9	87.2	257.1	257.1
325.7	68.6	68.6	49.0	51.4	51.4
342.9	34.3			205.7	
D_{Min}	24.2°	24.2°	28.1°	30.4°	30.4°

REFERENCES

No.	Author	Title, etc
1	J.G. Walker	Circular orbit patterns providing continuous whole Earth coverage. RAE Technical Report 70211 (1970)
2	J.G. Walker	Some circular orbit patterns providing continuous whole Earth coverage. *J. Brit. Interplanetary Soc.*, 24, 369-384 (1971)
3	J.G. Walker	Continuous whole Earth coverage by circular orbit satellites. *Satellite systems for mobile communications and surveillance*, IEE Conference Publication 95, 35-38 (1973) [Also available as RAE Technical Memorandum Space 194 (1973)]
4	J.G. Walker	Continuous whole-Earth coverage by circular-orbit satellite patterns. RAE Technical Report 77044 (1977)
5	J.G. Walker	Satellite patterns for continuous multiple whole-Earth coverage. *Maritime and aeronautical satellite communication and navigation*, IEE Conference Publication 160, 119-122 (1978)
6	J.G. Walker	RAE coverage studies relevant to 18-satellite constellations. Unpublished RAE Note dated 20 May 1980
7	J.G. Walker	Single-satellite-per-plane patterns potentially suitable for GPS. Unpublished RAE Note dated 18 July 1980
8	J.E. Draim	Geometrically derived orbital constellations : methodology and GPS applications. Unpublished conference contribution, 5-6 June 1980
9	K. Critchlow	*Order in space : a design source book.* London, Thames and Hudson (1969); New York, Viking Press (1970)
10	S.A. Book W.F. Brady P.K. Mazaika	The nonuniform GPS constellation. *Position location and navigation symposium*, IEEE PLANS 80, 1-8,(1980)
11	G.V. Mozhaev	The problem of continuous earth coverage and kinematically regular satellite networks. II. *Kosmich. Issled.*, 11, 1, 59-69 (1973) [Translated in *Cosmic Research*, 11, 1, 52-61 (1973)]
12	A.H. Ballard	Rosette constellations of Earth satellites. *IEEE Trans. Aerosp. Electron. Syst.*, 16, 5, 656-673 (1980)
13	P.S. Jorgensen	Navstar/Global Positioning System 18-satellite constellations. *Navigation : J. Inst. Nav.*, 27, 2, 89-100 (1980)
14	J.M. Blake	Modified rosette constellations. Unpublished conference contribution, 5-6 June 1980

REFERENCES (concluded)

No.	Author	Title, etc
15	P.S. Jorgensen	Navstar Global Positioning System 18-satellite constellations. Unpublished conference contribution, 5-6 June 1980
16	W.F. Brady P.S. Jorgensen	Worldwide coverage of the Phase II Navstar satellite constellation. *Navigation : J. Inst. Nav.*, 28, 3, 167-177 (1981)

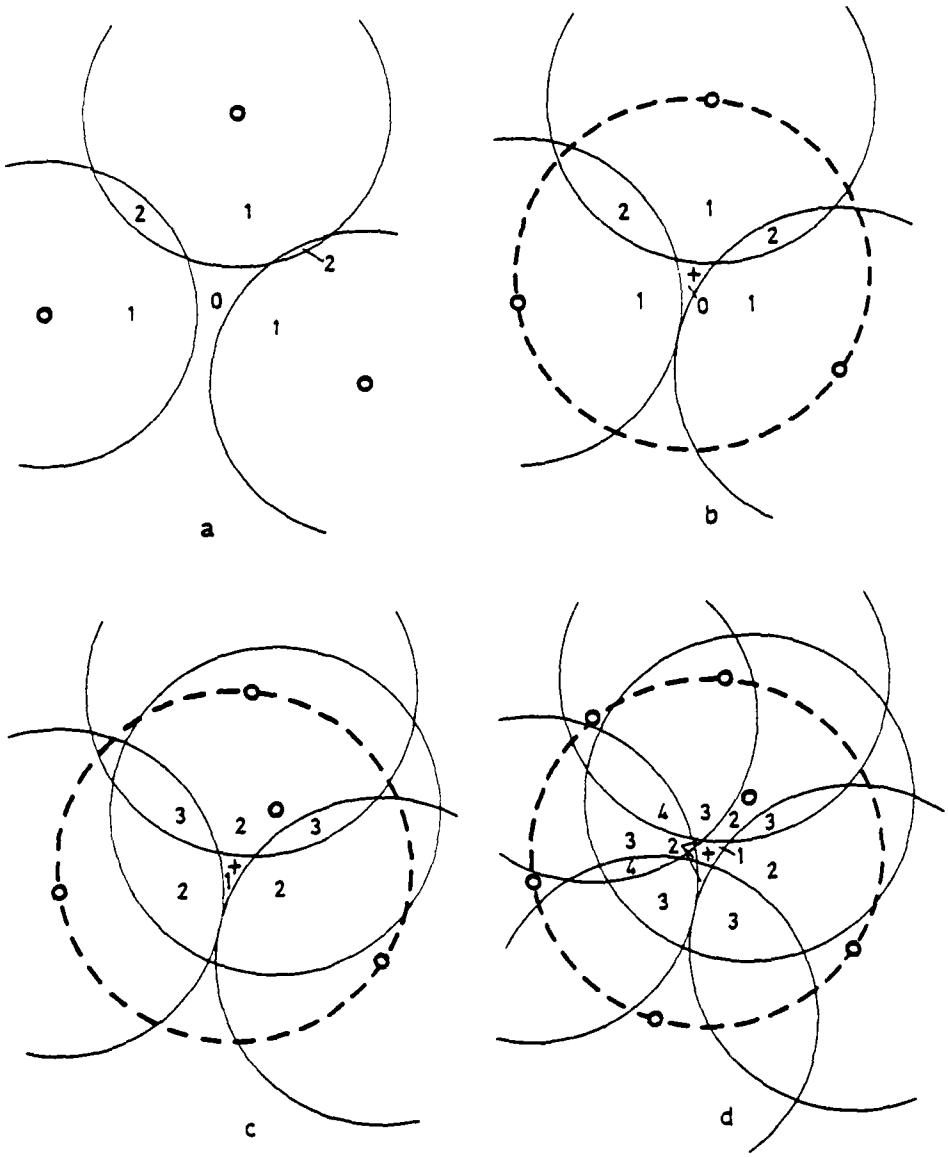

Fig 1a-d Circumcircle centre as locally critical point

TR 82116

Fig 2a-c

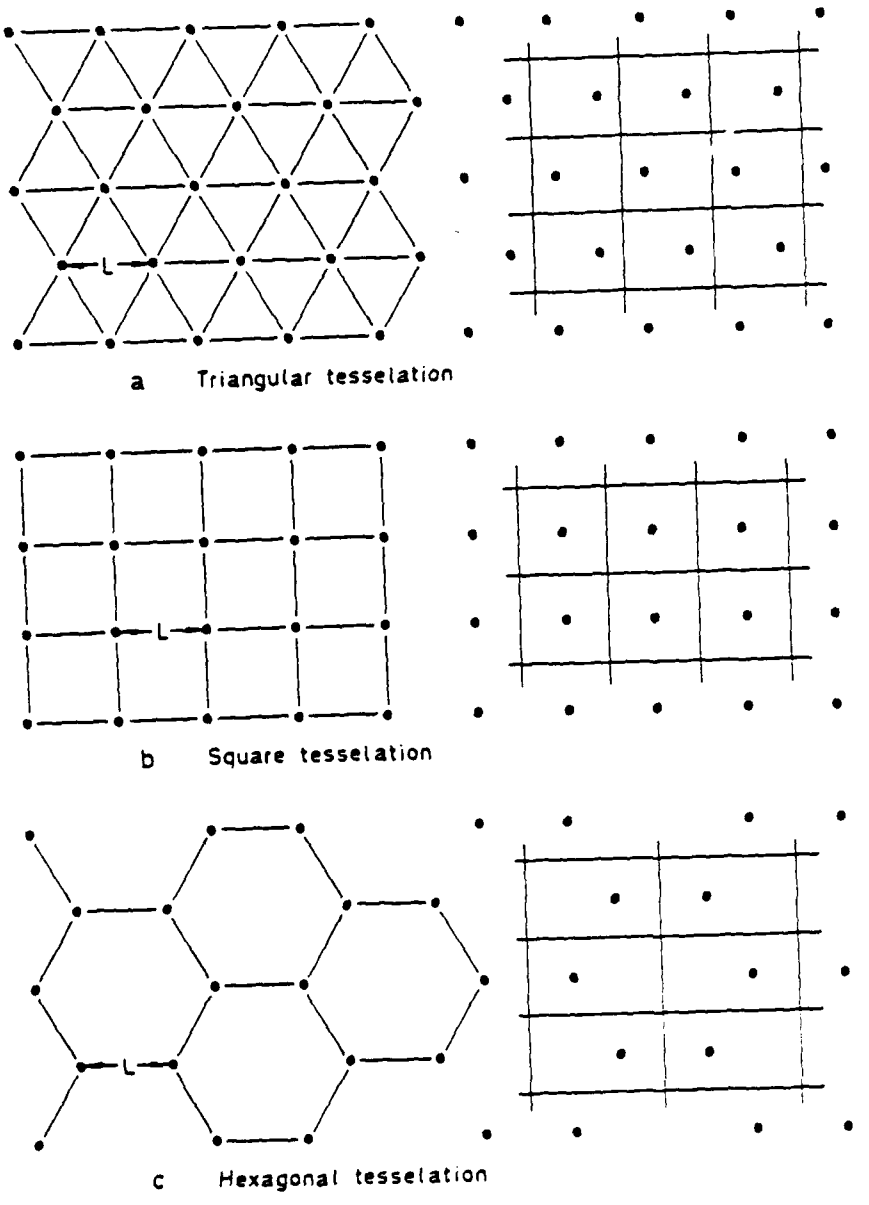

Fig 2a-c Regular tesselations

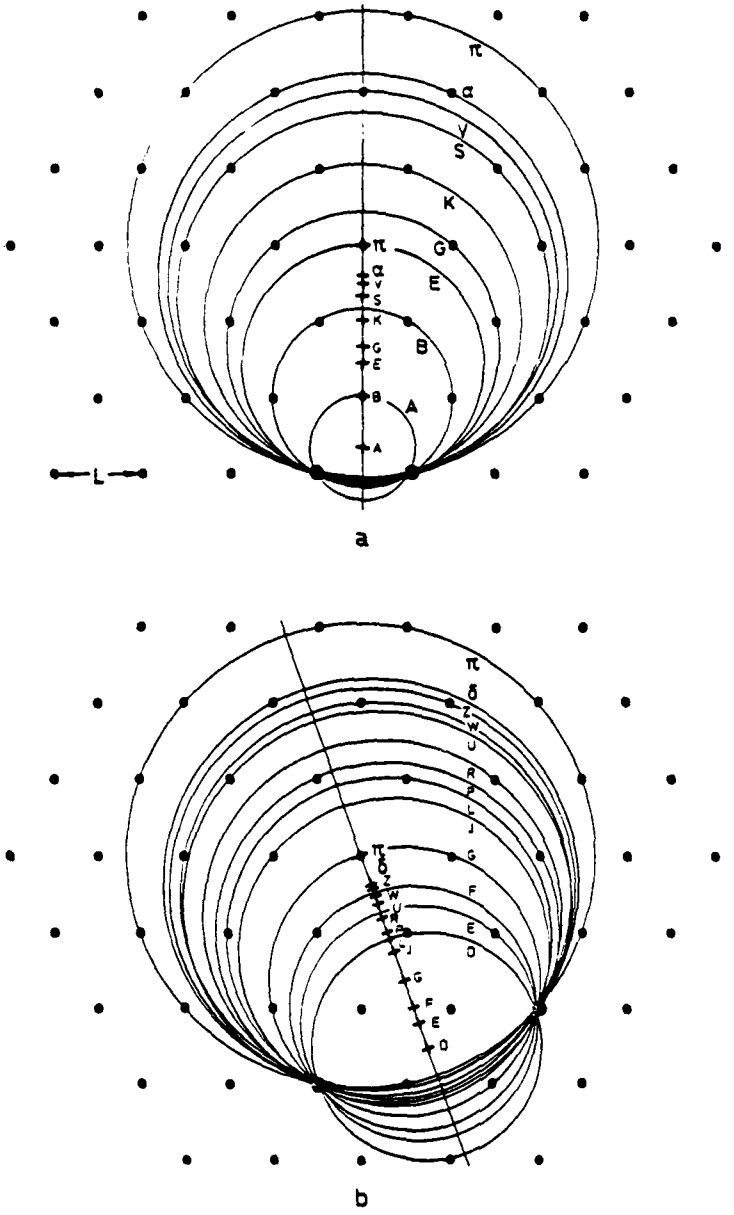

Fig 3a&b Finding values of R for triangular tesselation

Fig 4

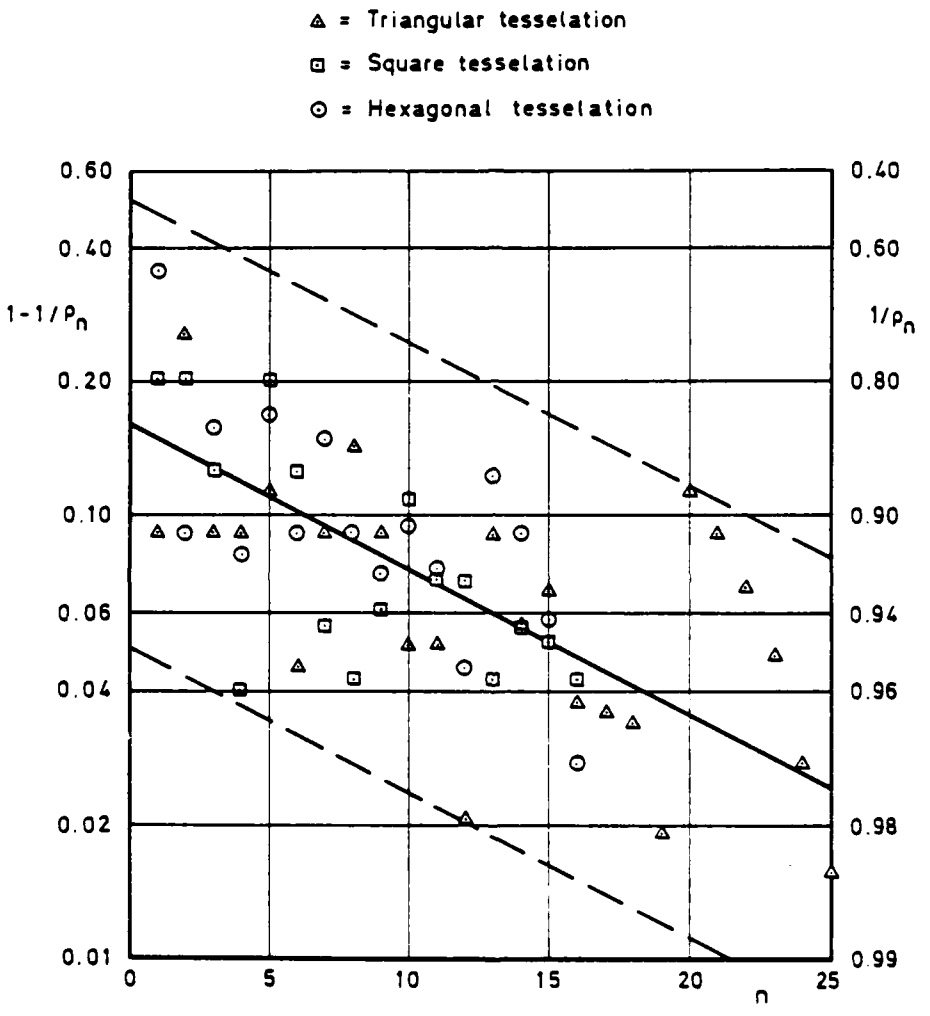

Fig 4 Semi-log plot of $1/\rho_n$ v n for regular tesselations

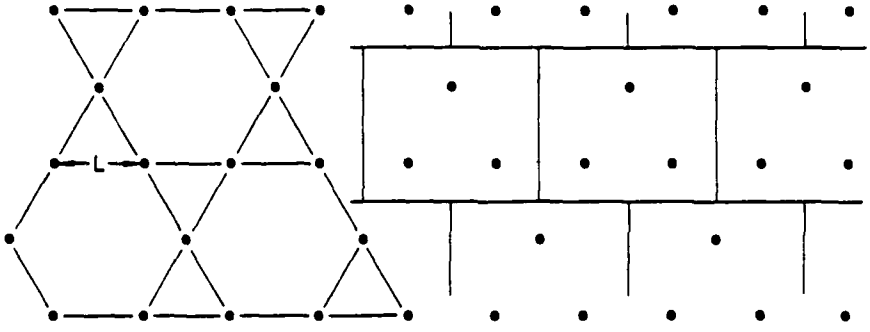

a Tri - hex A tesselation

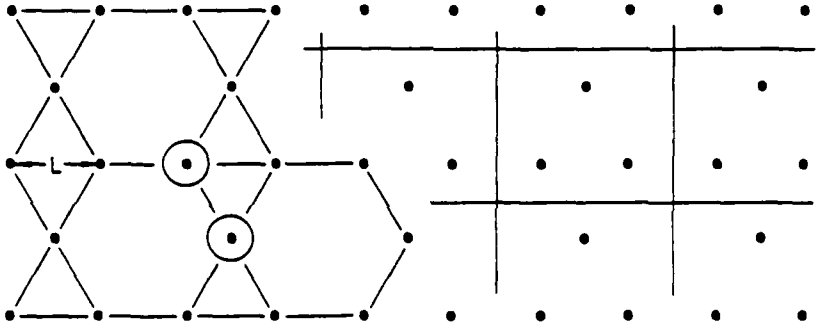

b Tri - hex B tesselation

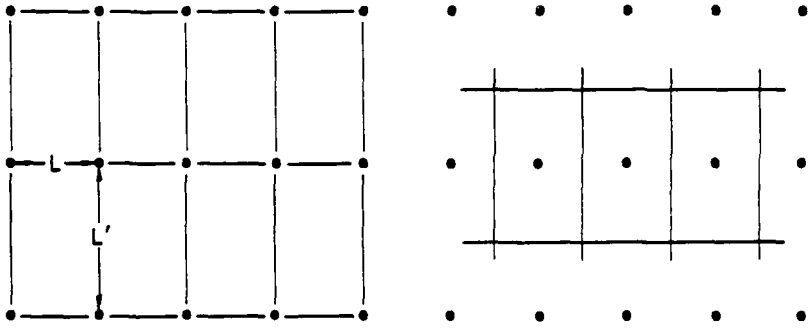

c Rectangular tesselation

Fig 5a-c Other tesselations

Fig 6

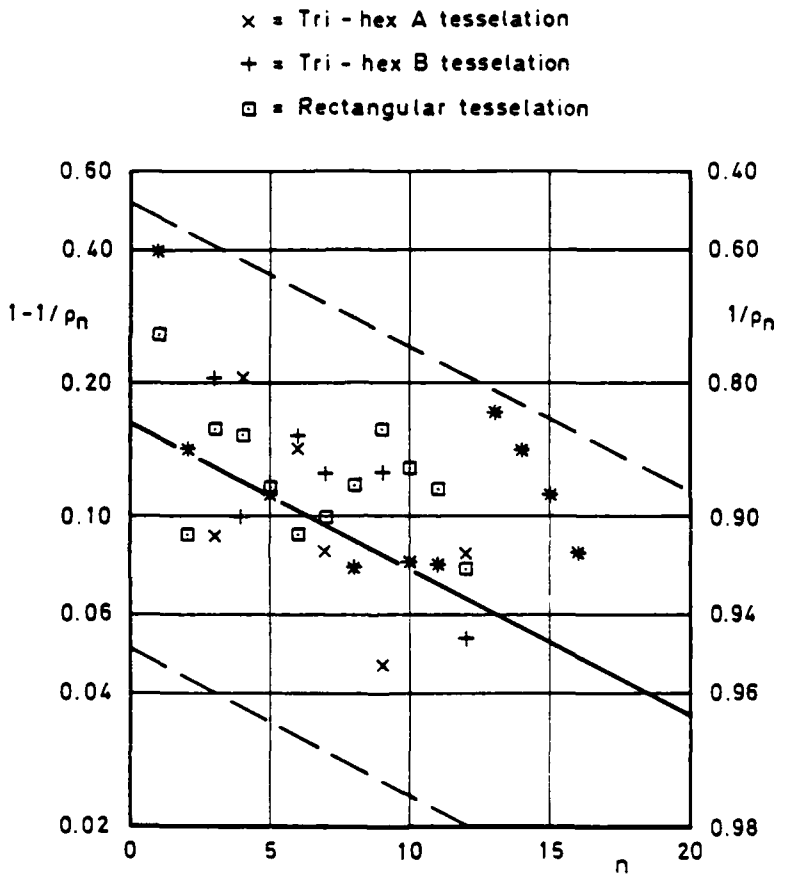

Fig 6 Semi-log plot of $1/\rho_n$ v n for other tesselations

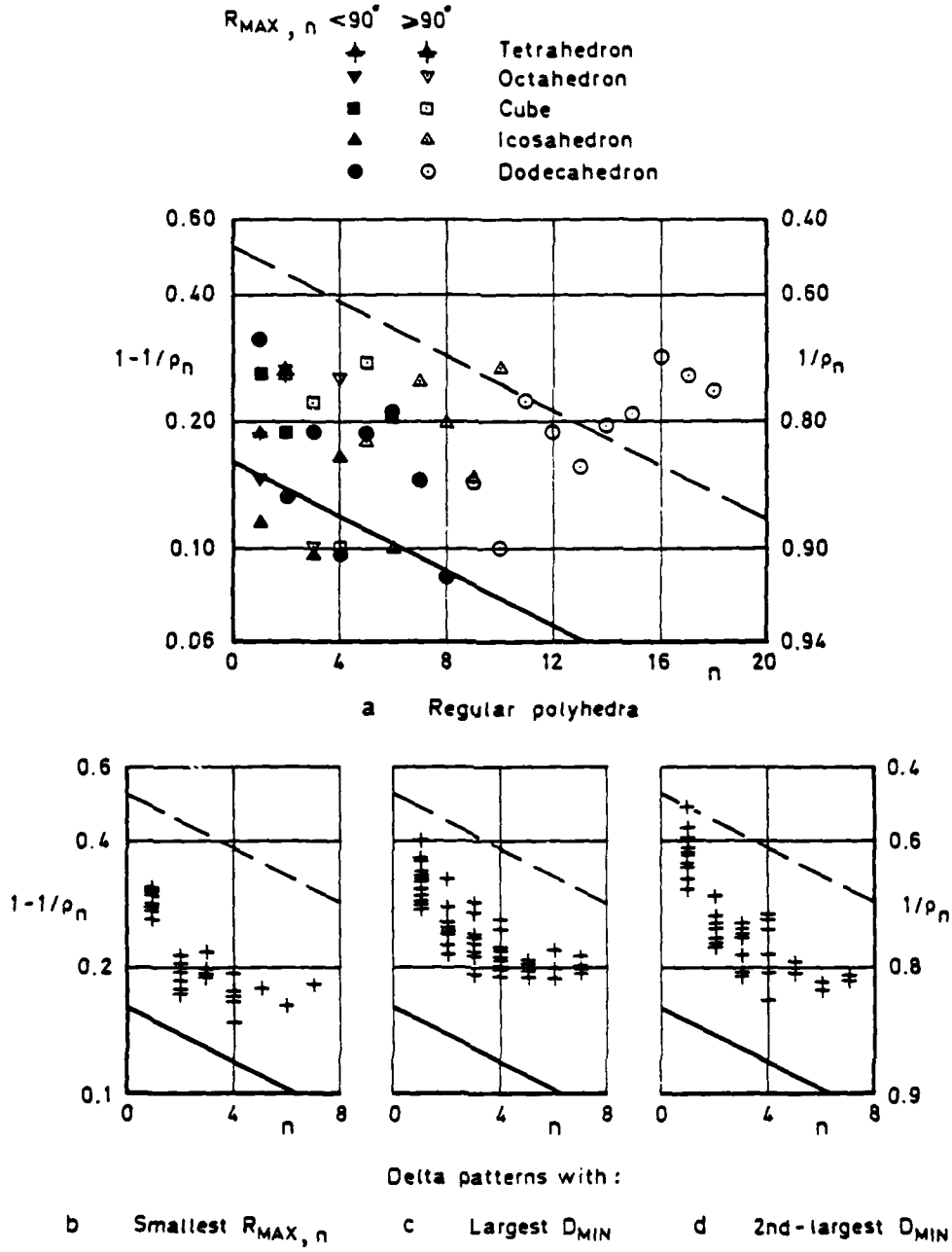

TR 82116

Fig 7a-d Semi-log plots of $1/\rho_n$ v n for spherical constellations

Fig 8

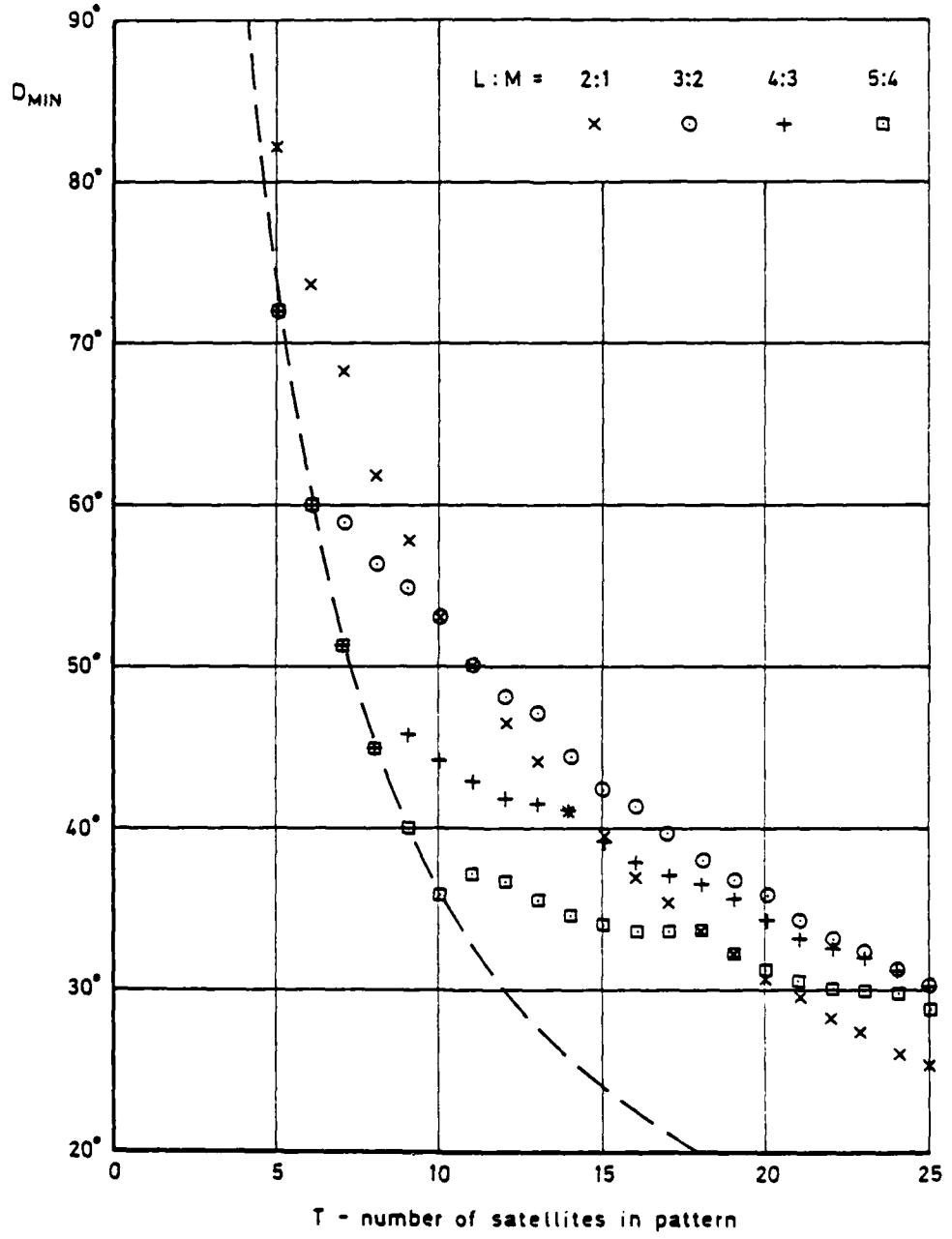

Fig 8 Largest values of D_{MIN} for delta patterns

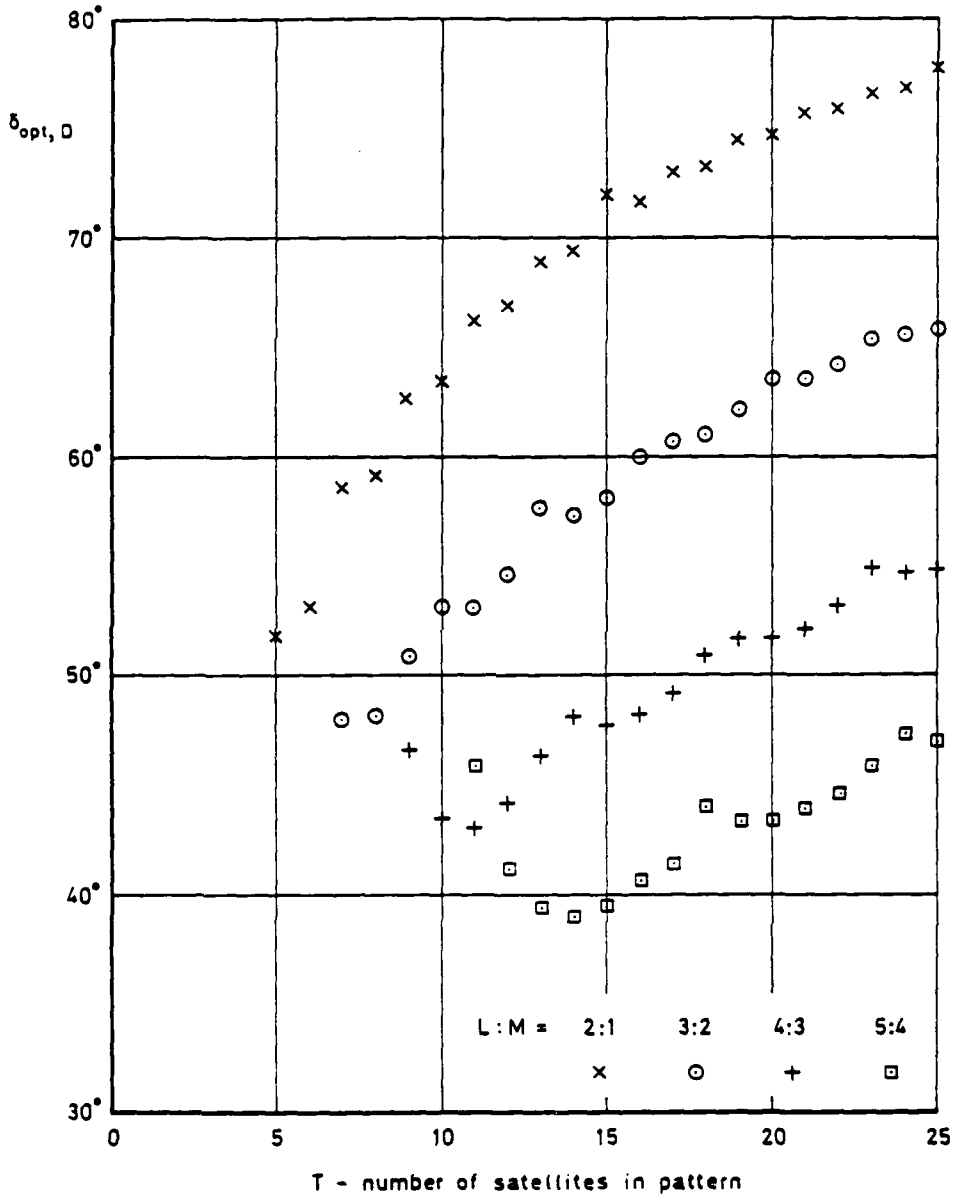

Fig 9 Inclinations for delta patterns giving largest values of D_{MIN}

TR 82116

Figs 10&11

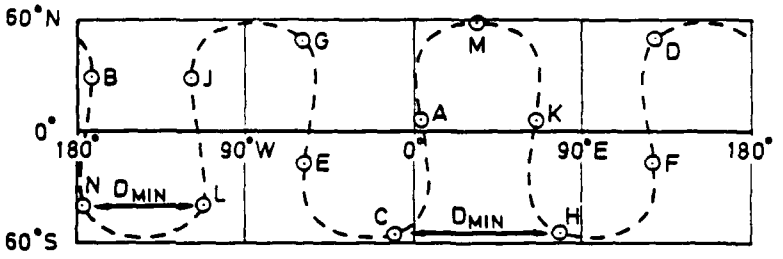

Fig 10 D_{MIN} for pattern 13/13/5, at ϕ = 1.0, showing Earth-track in 16-hour orbit (L:M = 3:2)

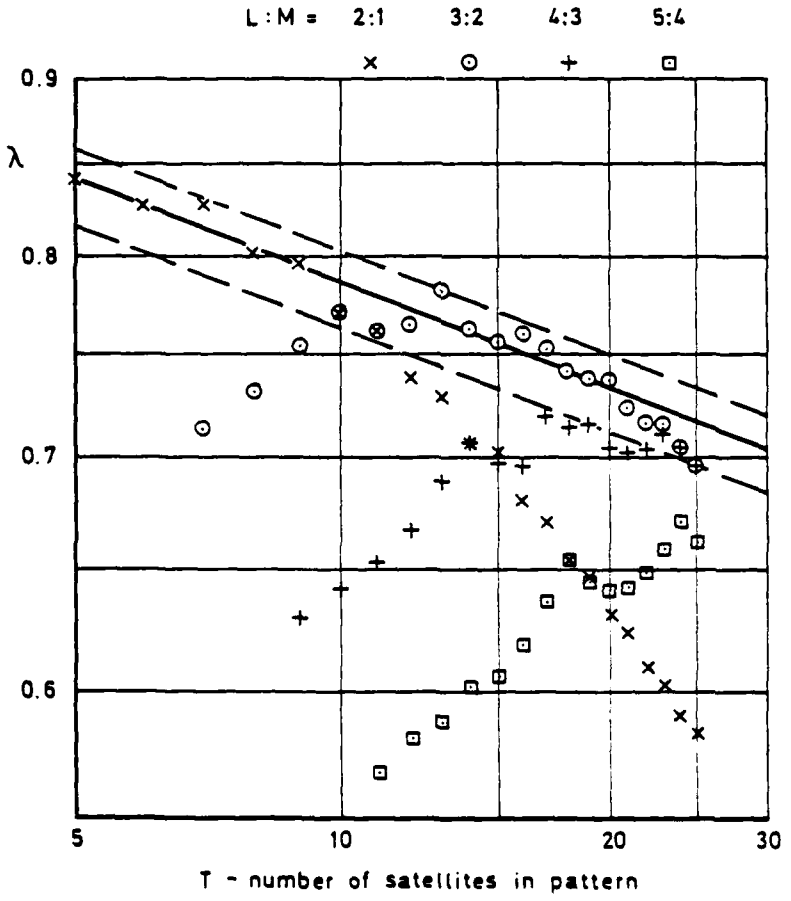

Fig 11 Log-log plot of λ v T for delta patterns giving largest values of D_{MIN}

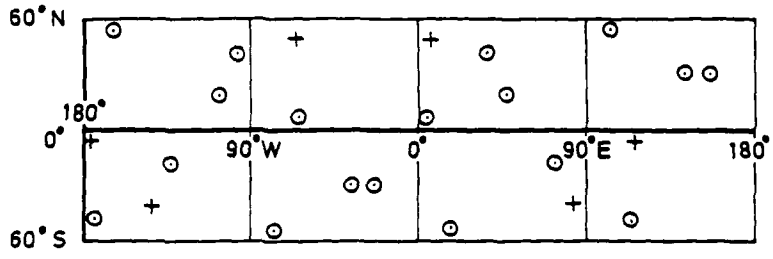

a Pattern 24/3/2 (⊙ and +) and non - uniform 18 - satellite pattern (⊙)

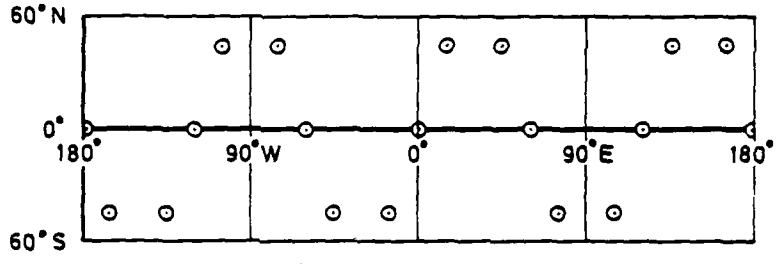

b Pattern 18/3/0

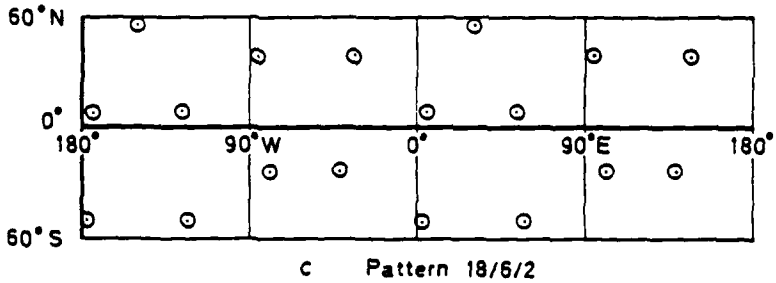

c Pattern 18/6/2

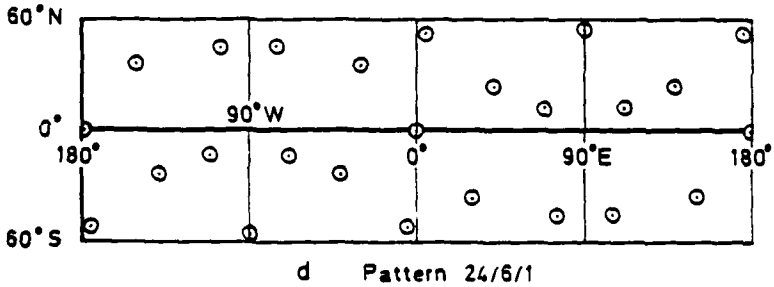

d Pattern 24/6/1

Fig 12a-d 18-satellite and 24-satellite delta patterns

Fig 13a-e

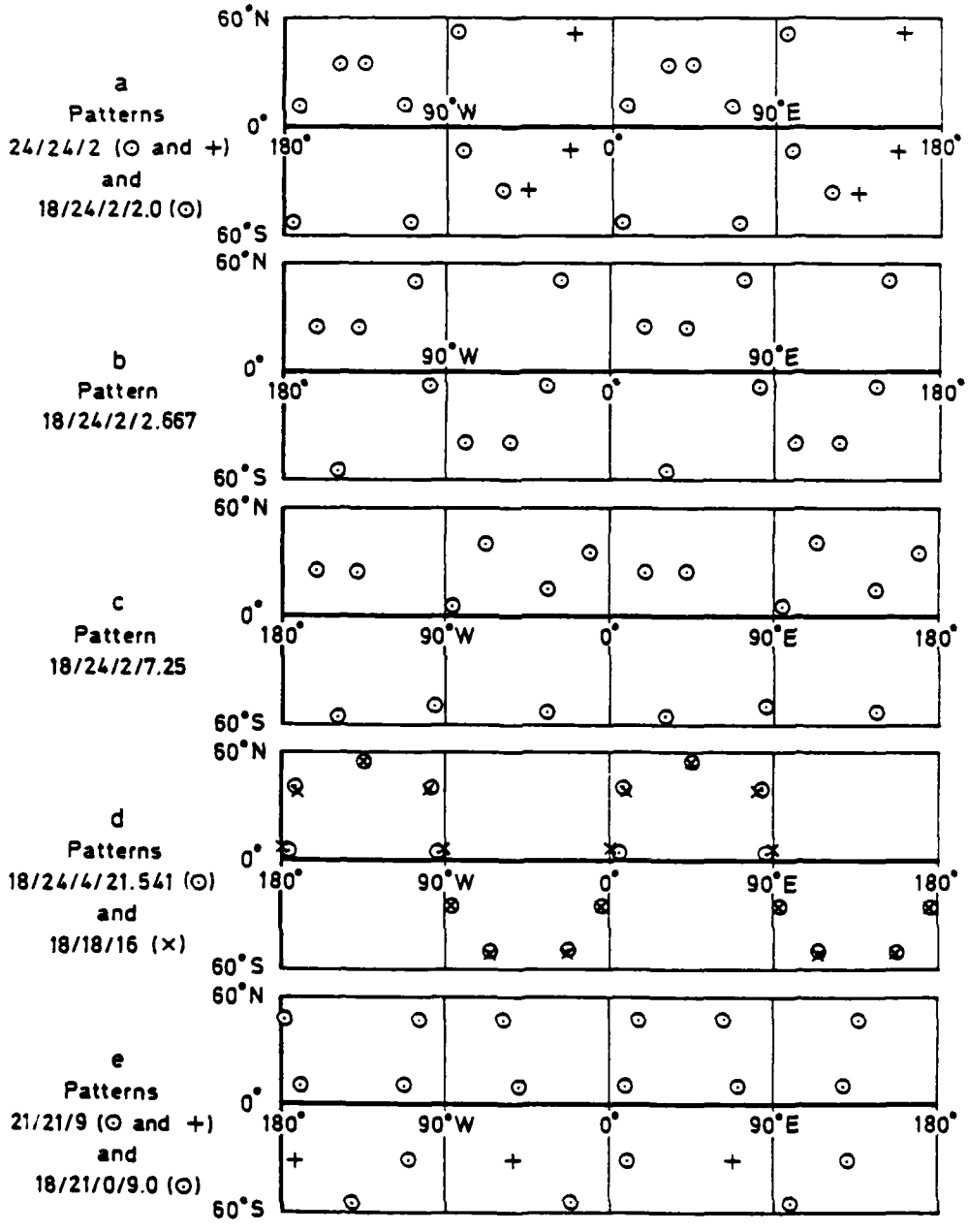

Fig 13a-e 18-satellite omega patterns

REPORT DOCUMENTATION PAGE

UNLIMITED

UNLIMITED

END

DATE
FILMED

8-83

DTIC